doi:10.1016/j.ymthe.2004.12.017

phoid lines exposed to Adv5-SV-DNE1 (Fig. 3A). The marked decrease in wtEBNA1 expression by mtEBNA1 transduction could represent elimination of rEBV episomes from a considerable fraction of cells, although the possibility that wtEBNA1 expression was down regulated by mtEBNA1 cannot be excluded at this step.

To investigate whether mtEBNA1 inhibits rEBV episome maintenance in cells, we quantified viral genomic DNA loads sequentially by real-time PCR after Adv inoculation. We exposed NU-GC-3/rEBV cells to Adv likewise and then cultured them in the absence of G418. rEBV genome loads in Adv5-CV-DNE1-exposed cells began to decrease 3 days postinoculation and were considerably reduced to 11% of the Adv5-CV-LacZ-exposed control 9 days postinoculation (Table 2). In contrast, the dynamics of viral genome loads in Adv5-CV-LacZ inoculation was unchanged throughout the observation (Table 2). Immunofluorescent staining consistently showed that more than 98% of cells exposed to Adv5-CV-LacZ, or mock infected, were positive for wtEBNA1 26 days after removal of G418 from culture (data not shown), indicating that spontaneous loss of the rEBV genome was not frequent, even in G418-free culture during the test period. Reduction of rEBV loads by mtEBNA1 transduction occurred in Akata$^-$/rEBV cells [14] as well (a decrease to 19% of the LacZ control, Table 2; for mtEBNA1 expression, see Fig. 3A). Thus, our mtEBNA1, as a dominant-negative EBNA1, can efficiently eradicate viral episomes from cells, at least at the bulk-culture level.

dnEBNA1-Induced Eradication of EBV Episomes at Single-Cell Level in Different EBV Latency Programs and Tissue Origins

We then examined whether dnEBNA1 could efficiently eradicate EBV episomes (multicopies per cell) at the single-cell level by *in situ* hybridization for EBV-encoded small RNA 1 (EBER1-ISH) using rEBV-converted cell lines, since our previous study [39] demonstrated that an EBER expression status correlates well with the rEBV genome persistence/loss in converted cells. Adv5-SV- (or -CV)-DNE1 also successfully expressed dnEBNA1 protein at substantial levels in the other converted lines, MT-2/rEBV (T cell) [40] and BJAB/rEBV (B cell) [41] (Fig. 3A; the decrease in wtEBNA1 levels should also be noted), which display EBV latency types II and III, respectively (Table 1). EBER1-ISH showed that 89 ± 3% of NU-GC-3/rEBV cells (Fig. 3B), 77 ± 5% of Akata$^-$/rEBV cells, 80 ± 6% of BJAB/rEBV cells, and 85 ± 3% of MT-2/rEBV cells in the absence of G418 appeared to be negative for EBER1 9 days after a single inoculation with Adv5-SV- (or -CV)-DNE1. These reproducible findings were reflected also by looking at the growth kinetics of rEBV-converted cell lines in the presence of G418. The experimental concept is based on the premise that cells that lose rEBV (rEBV-lost cells) cannot survive in G418-containing culture [38,39]. The Adv5-SV (or -CV)-DNE1-exposed cultures showed obvious, albeit transient, suppression of cell proliferation 4 to 6 days postinoculation, whereas Adv5-SV (or -CV)-LacZ-exposed cells as well as mock-infected controls continued to grow steadily (Fig. 3C). The loss of resistance to G418 cytotoxicity occurred dose dependently upon addition of Adv5-DNE1, and the maximal growth inhibition achieved by a single Adv5-DNE1 inoculation was almost equal among all the converted cell lines. The viability was 9–23% of the corresponding Adv5-LacZ-inoculated controls (Fig. 3C) and is largely consistent with the ability of Adv's to infect the convertants (Table 1). After the "nadir" of cell viability, as was typically seen in NU-GC-3/rEBV, dnEBNA1-transduced cultures were liberated from growth suppression 6 days after a single Adv inoculation (Fig. 3C), representing a proliferation of cells that still carried rEBV, i.e., cells not transduced with the dnEBNA1 gene. When we reexposed cells to Adv5-SV-DNE1 4 days after the first inoculation, their growth was more affected (Fig. 3C).

The results indicated overall that our dnEBNA1 did eliminate multiple rEBV episomes almost completely at the single-cell level from individual cells into which dnEBNA1 was successfully transduced, in any major viral latency and in different cell backgrounds.

TABLE 2: Reduction of rEBV genomic loads by mtEBNA1 transduction

Cells	Inoculation	EBV genome number per cell[a] (days after Adv inoculation)				
		0	3	6	9	12
NU-GC-3/rEBV	Mock	1.9 ± 0.36	1.9 ± 0.20	1.8 ± 0.29	1.8 ± 0.26	NT
	Adv5-CV-LacZ		1.8 ± 0.12	1.7 ± 0.18	1.8 ± 0.11	NT
	Adv5-CV-DNE1		0.9 ± 0.12	0.3 ± 0.23	0.2 ± 0.04	NT
Akata$^-$/rEBV	Mock	26.7 ± 3.2	24.8 ± 1.2	25.0 ± 0.8	26.6 ± 1.2	25.4 ± 1.9
	Adv5-SV-LacZ		26.1 ± 2.5	28.0 ± 2.6	28.3 ± 1.7	24.9 ± 2.1
	Adv5-SV-DNE1		22.3 ± 0.6	15.8 ± 2.2	5.0 ± 0.3	6.1 ± 0.7
Namalwa[b]	–	2.0 ± 0.08				
BJAB[b]	–	0				

[a] Viral genome copies per cell were quantified by the real-time PCR assay after Adv-mediated mtEBNA1 transduction. In the experiments, G418 was removed from culture 7 days before Adv inoculation, and 0.1 mM acyclovir (an inhibitor of viral genome amplification during the lytic cycle) was added to the culture 3 days before Adv inoculation (m.o.i. of 20) to prevent overestimation of latent viral episome number, which may be caused by the possibly occurring spontaneous viral lytic cycle. Data indicated are averages ± SD of results from three experiments. NT, not tested.

[b] Namalwa [65] and BJAB cells served as EBV-positive and -negative controls, respectively, for each test, and the results were highly reproducible.

Therapeutic Potential of dnEBNA1 Against Naturally EBV-Infected BL Cells

We assessed dnEBNA1 for its ability to inhibit the growth of naturally EBV-infected BL tumor cells in association with the enforced loss of resident viral episomes using Mutu I [42] and Akata-EC (early cultured) cells [17]. We selected these BL cells as test cells because (1) EBV-lost clones of Mutu I cells can be isolated spontaneously or by chemical treatment (at a low frequency) and can still survive, although these clones reportedly exhibit impaired growth [16,43], and (2) the survival/growth of Akata-EC cells strongly depends on the existence of EBV [17]. After Adv5-SV-DNE1 inoculation at an optimal m.o.i., dnEBNA1 protein was expressed in Mutu I cells at significant levels and in Akata-EC cells at a detectable level but at a level noticeably lower than in the Mutu I cells (Fig. 4A). The expression of wtEBNA1 was clearly decreased in the Mutu I cells (Fig. 4A), as seen in rEBV-converted cells (Figs. 2 and 3A). In contrast, unexpectedly, the wtEBNA1 expression level in Akata-EC cells exposed to Adv5-SV-DNE1 remained unchanged (Fig. 4A). Consistently, quantitative PCR assay showed that EBV DNA loads decreased significantly in the Mutu I cells, but were almost unchanged in Akata-EC cells after exposure to Adv5-SV-DNE1. The virus genome copy numbers per Mutu I cell after 6 days were 11.2 ± 4.6 following Adv5-SV-DNE1 inoculation vs 39.8 ± 3.5 in Adv5-SV-LacZ inoculation controls and 42.0 ± 2.6 in mock-inoculated cells ($P < 0.01$). However, successive viable cell counts monitored in parallel revealed that Adv5-SV-DNE1 significantly suppressed the growth of both Mutu I and Akata-EC BL lines in a dose-dependent fashion, compared with Adv5-SV-LacZ-inoculated cells ($P < 0.001$) (Fig. 4B). These results suggest that most EBV-lost Mutu I cell clones were still living but underwent profound growth retardation [16,43], whereas Akata-EC clones were more likely to have been predisposed to immediate cell death rather than growth arrest after EBV was eradicated [17].

To corroborate that dnEBNA1 truly eradicated EBV episomes from naturally EBV-positive BL cells at the single-cell level, we exposed Mutu I cells to Adv's for the picornavirus intraribosomal entry site (IRES)-mediated coexpression of dnEBNA1 or LacZ with hygromycin B resistance (*hyg*^{r}), i.e., Adv5-SV-DIH or -LIH (Fig. 4C; for designation of Adv's, see Materials and Methods), and then cultured them in the presence of hygromycin B to grow selectively cells expressing dnEBNA1 or LacZ (the selection conditions are detailed in the legend to Fig. 4D). The fluorescence *in situ* hybridization (FISH) assay demonstrated that >96% of Adv5-SV-DIH-inoculated/hygromycin B-selected viable Mutu I cells were negative for EBV genomic signals 10 days after Adv inoculation (Fig. 4D, bottom left), whereas ≤0.3% of Adv5-SV-LIH-inoculated/hygromycin B-selected viable cells were negative for these signals (Fig. 4D, bottom middle) ($P < 0.001$ by t test). These results signify that individual cells that were transduced with dnEBNA1 lost multiple copies of the EBV episome. Without hygromycin B treatment, 59% of the Mutu I cells in Adv5-SV-DIH-inoculated culture were negative for FISH signals (Fig. 4D, top middle) vs 0.4% in Adv5-SV-LIH-inoculated culture (Fig. 4D, top right) ($P < 0.001$) 10 days after Adv inoculation, indicating that the positive selection worked well. In contrast, FISH-negative cells were detected only in a small population (≤7%) of Akata-EC cells after Adv5-SV-DNE1 inoculation, which was compatible with the results of immunoblots (Fig. 4A) and quantitative PCR assays (see above). In cell-sorting experiments, as expected, sufficient viable Akata-EC cells for analysis were obtained from Adv5-SV-LIH-inoculated/hygromycin B-selected control culture, but not from Adv5-SV-DIH-inoculated/hygromycin B-selected culture, suggesting again that most EBV-lost Akata-EC clones by dnEBNA1 were not able to survive [17].

Influence of dnEBNA1 on EBV-Uninfected Cells

We further examined whether dnEBNA1 would cause any adverse effects on EBV-uninfected nonmalignant cells (i.e., the human fibroblasts, MRC-5) and pairs of EBV-negative tumor lines and their virus convertants. Inoculation of MRC-5 with the fiber-substituted Adv5 vector [36] Adv5/35f-CV-DNE1 gave rise to dnEBNA1 expression levels consistent with a high efficiency of gene transfer (~75% of cells, Table 1) sufficient to assess the effects of dnEBNA1 on cell growth (Fig. 5A, left). MRC-5 cells inoculated with Adv5/35f-CV-DNE1 did not differ in growth characteristics from the Adv5/35f-CV-LacZ-inoculated control ($P = 0.386$) (Fig. 5A, right). Similarly in the EBV-negative NU-GC-3 line, Adv5-CV-DNE1 inoculation caused no significant difference in growth compared with the control Adv5-CV-LacZ inoculation ($P = 0.846$) (Fig. 5B, left). On the other hand, in the rEBV-convertant NU-GC-3/rEBV line, Adv5-CV-DNE1 inoculation significantly suppressed growth in comparison with Adv5-CV-LacZ inoculation ($P < 0.01$) (Fig. 5B, right). This growth suppression was considered to be attributable to dnEBNA1-induced eradication of rEBV, rather than cytotoxicity induced by dnEBNA1 per se, because dnEBNA1-transduced NU-GC-3/rEBV (with >90% of cells that lost rEBV, as shown in Fig. 3B) revealed a growth pattern similar to that of its parental (virus-negative) NU-GC-3 cell line (Fig. 5B, left). Consistent with these data is our previously reported result [15] that the growth of NU-GC-3 cells is promoted by conversion with rEBV. Transduction of dnEBNA1 did not affect the growth of other EBV-negative cell lines such as Akata$^-$ and BJAB (data not shown).

Suppressive Effect of dnEBNA1 on Tumor Growth/Induction *in Vivo*

Finally, we examined the *in vivo* effects of dnEBNA1 using an animal xenograft model. When subcutaneous

doi:10.1016/j.ymthe.2004.12.017

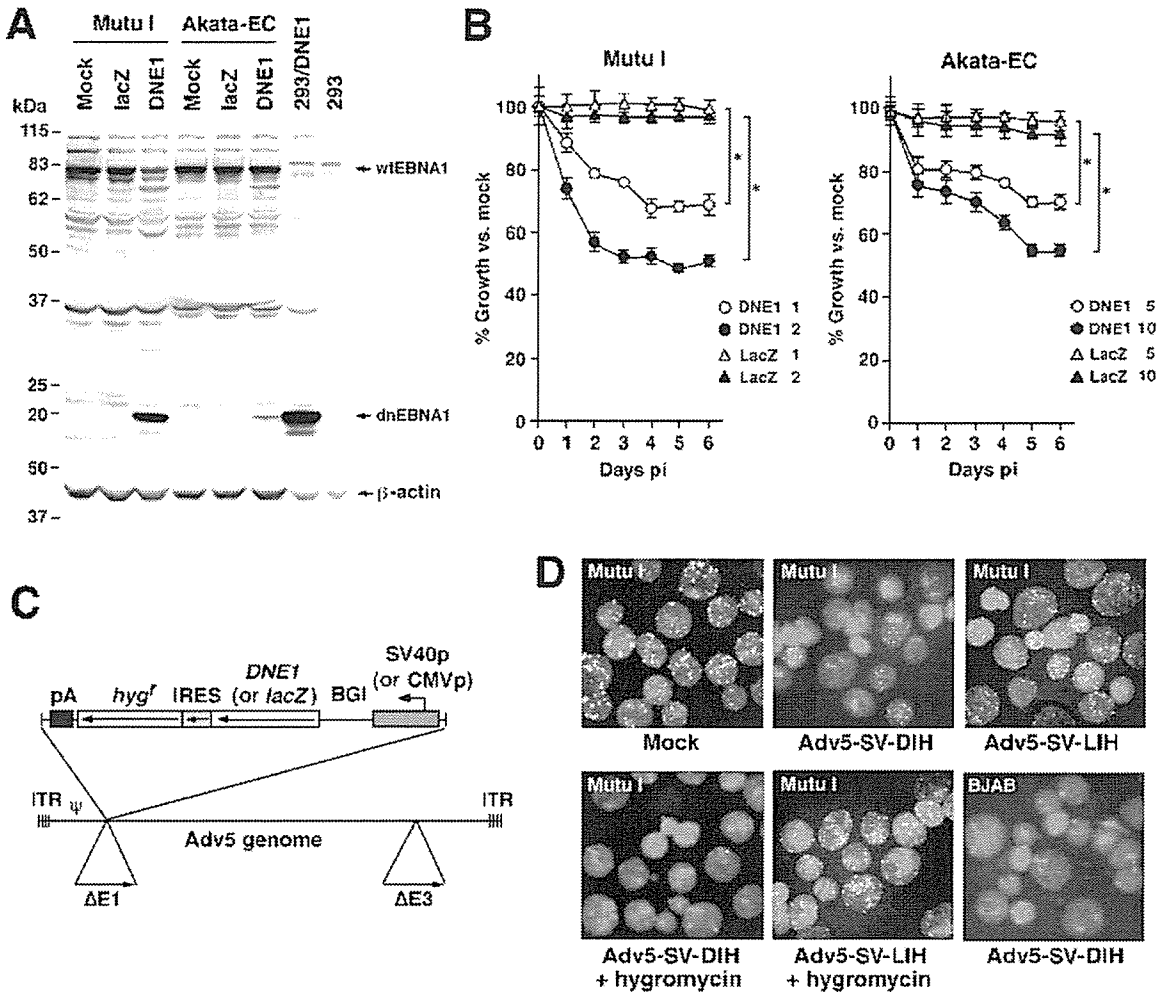

FIG. 4. Effects of dnEBNA1 on naturally EBV-positive BL tumor cells. (A) Immunoblot analysis of dnEBNA1 transduction. Applied m.o.i. of Adv5-SV-DNE1 or -LacZ were 2 for Mutu I and 10 for Akata-EC. 293/DNE1 indicates a positive control for dnEBNA1 expression. Expression of wtEBNA1 and dnEBNA1 (top), along with that of β-actin as an internal control (bottom), was assayed at 4 days after Adv inoculation. Molecular size standards are indicated on the left. (B) Cell proliferation assay. Mutu I or Akata-EC cells were inoculated with Adv's, at different m.o.i. as indicated by the symbols, and their growth was followed by WST-1 assay, which was started 5 h after Adv inoculation (Day 0). Results are expressed as a percentage of absorbance values of Adv5-SV-DNE1- (circles) or Adv5-SV-LacZ-inoculated cultures (triangles) against the absorbance of the mock-infected control on each day. DNE1 2, for example, represents inoculation with Adv5-SV-DNE1 at an m.o.i. of 2. Each symbol with a bar represents mean ± SD of the absorbance percentages obtained from the experiments repeated three times. ANOVA showed significant main effects of Adv-DNE1 inoculation (*). Post hoc Dunnett test revealed a significant decrease in percentage values against mock-infected cells in cells inoculated with Adv5-SV-DNE1 at both m.o.i. (C) Adv construct for bicistronic gene expression. The genome structure of Adv5-SV (or -CV)-DIH (or -LIH) used to sort gene-transduced cells is schematically shown. BGI, β-globin intron sequence; IRES, intraribosomal entry site; ITR, adenoviral inverted terminal repeat; ψ, packaging signal; pA, poly(A) signal; ΔE1 and ΔE3, deleted genes in the vector genome [35]. (D) FISH analysis of EBV genome. Data from a series of Mutu I cells are shown. Adv5-SV-DIH and -LIH denote inoculations with Adv's for dual expression of dnEBNA1 or LacZ, respectively, along with *hygr* as the selective marker. Mutu I, Adv5-SV-DIH + hygromycin and Mutu I, Adv5-SV-LIH + hygromycin denote cultures that were inoculated with Adv (m.o.i. of 2) and then treated with hygromycin B (400 μg/ml) to remove cells that had not been transduced with the genes. Hygromycin B was added to culture on the day following Adv inoculation, and then cells were cultivated for 4 consecutive days. The resultant surviving cells were propagated in the absence of hygromycin B for a further 5 days and screened for EBV infection by FISH. Mutu I, Adv5-SV-DIH and Adv5-SV-LIH denote cultures inoculated with Adv alone. Mutu I, Mock and BJAB, Adv5-SV-DIH served as EBV-positive and -negative controls, respectively. All samples were assessed 10 days postinoculation. Cells with green fluorescent dot signals are positive for the EBV genome. Original magnification: ×200.

tumors appeared in 24 flanks of 12 SCID mice tested after implantation of Mutu I cells (for details of procedure, see Materials and Methods)—usually at 9–11 days—we gave intratumoral injections with Adv5-SV-DNE1, Adv5-SV-LacZ, or phosphate-buffered saline (PBS) in 8 flanks each and observed the animals for up to 14 days after injection. During this time, all 8 tumors injected with Adv5-SV-DNE1 ceased to grow or

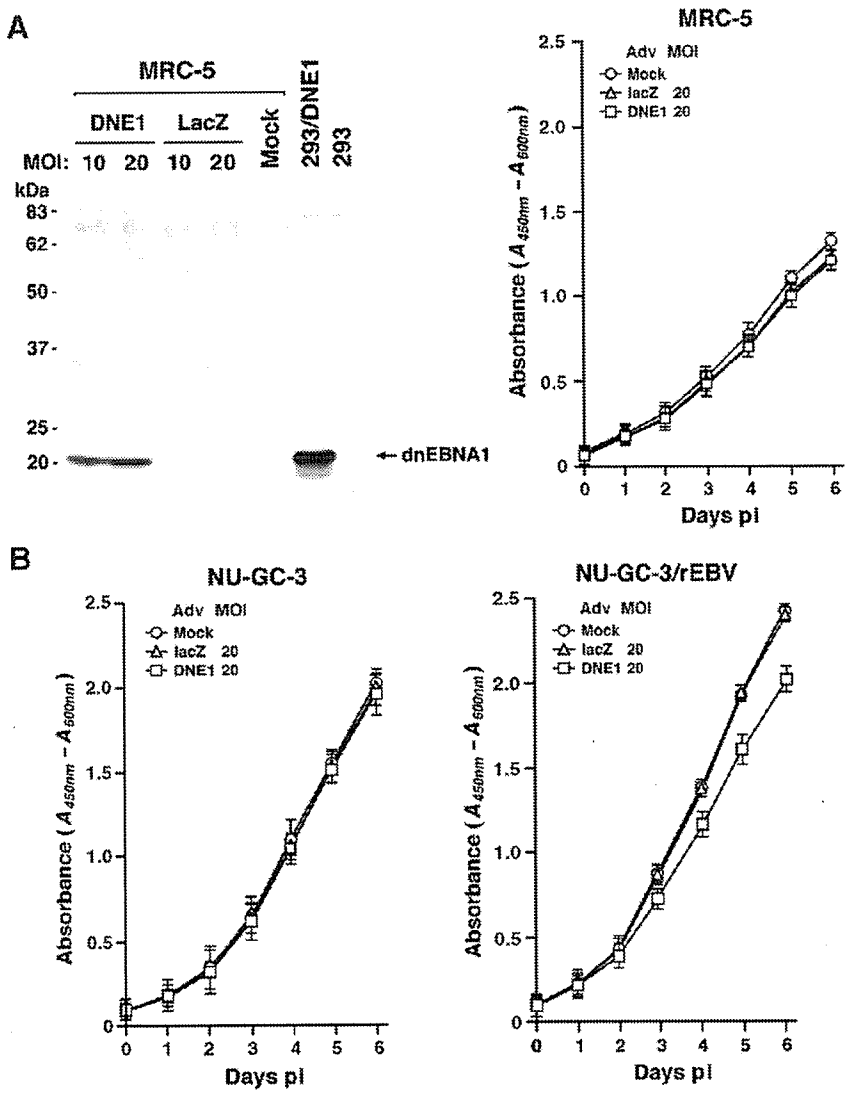

FIG. 5. Effects of dnEBNA1 on EBV-uninfected cells. (A) Adv-mediated dnEBNA1 expression and its effect on MRC-5 cell growth. MRC-5 cells were inoculated with Adv5/35f-CV-DNE1 or -LacZ at m.o.i. of 10 and 20 and analyzed by immunoblotting 3 days postinoculation (pi) (left). 293/DNE1 and 293 indicate the positive and negative controls, respectively. Molecular size standards are indicated at the left. Proliferation of MRC-5 cells (right) was measured by WST-1 assay after Adv5/35f-CV-DNE1 or Adv5/35f-CV-LacZ inoculation at the indicated m.o.i., compared with mock infection. Day 0 represents 5 h after Adv inoculation. Each symbol with a bar represents mean ± SD of the absorbance obtained from one of three experiments. Statistical analysis was carried out as done for Fig. 4B. (B) Proliferation of the NU-GC-3 line (left) and its rEBV-convertant NU-GC-3/rEBV (right) after dnEBNA1 transduction. Cells (6×10^2/well) were inoculated with Adv5-CV-DNE1 or Adv5-CV-LacZ at the indicated m.o.i. The substantial Adv-mediated expression of dnEBNA1 in both cell lines was as shown in Supplemental Fig. S1 and Fig. 2. Cell growth was measured by WST-1 assay in comparison with mock infection. Day 0 represents 5 h after Adv inoculation. Data are expressed as in (A) and were statistically analyzed as done for Fig. 4B.

regressed (1 tumor), whereas the 16 tumors injected with Adv5-SV-LacZ or PBS continued to grow aggressively (Fig. 6A). This was confirmed by the significant difference in tumor weights between the dnEBNA1-transduced mouse group and the control groups ($P < 0.001$ by Mann–Whitney U test) (Fig. 6B). EBER1-ISH and histological examinations showed that EBV-lost cells (~30%) and dead cells were present in the small tumors at the Adv5-SV-DNE1 inoculation sites, and the large tumors at the control sites were filled with viable EBER1-positive cells (data not shown). Another animal experiment revealed that implantation of Mutu I cells preinoculated with Adv5-SV-DNE1 did not induce tumors at all in all four tested flanks of mice, but implantation of cells preinoculated with Adv5-SV-LacZ induced tumors in all four implanted flanks that exceeded 2 cm in dimension by 14–20 days after cell injection (Fig. 6C). These results indicate that dnEBNA1 acts to suppress tumor growth *in vivo*.

Discussion

A previous study by others has shown that several EBNA1 derivatives are capable of interrupting the EBNA1-*ori*P functions, using an artificial system of *ori*P-carrying plasmids and cells transfected with the wtEBNA1 gene [34]. In the present study we have demonstrated that an EBNA1 mutant, with a similar domain constitution, eradicates EBV episomes efficiently from infected cells, therefore acting as dnEBNA1, irrespective of viral latency type and cell lineage (lymphoid and epithelial). In fact, transduction of dnEBNA1 yielded EBV-negative cell clones from naturally EBV-infected BL lines Mutu I and Daudi at a much

doi:10.1016/j.ymthe.2004.12.017

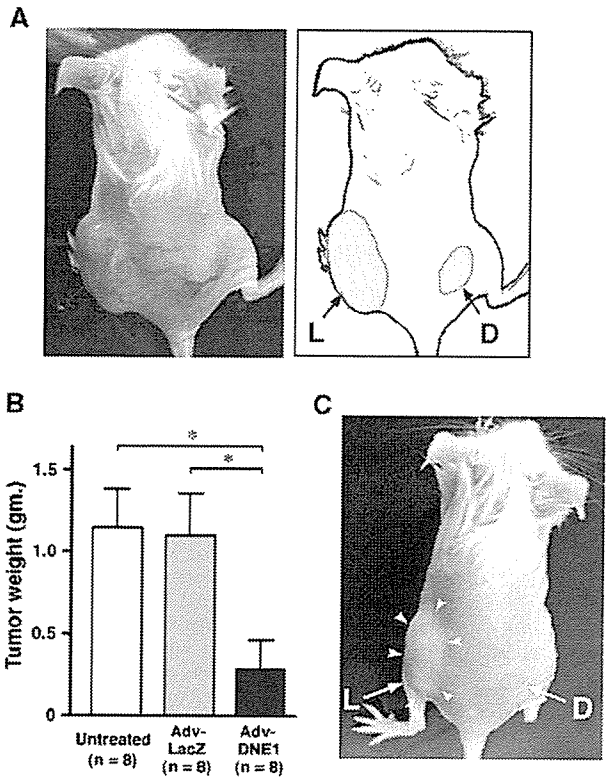

FIG. 6. Animal experiments. (A) Inhibition of tumor growth by dnEBNA1. Mutu I cells (1×10^7) were implanted subcutaneously in each flank of 12 SCID mice (i.e., 24 flanks). When tumors became palpable, at about 10 days after implantation, Adv's (10^8 pfu per dose) and PBS (mock) were injected into 8 tumors each. A representative result photographed 8 days after Adv inoculation (i.e., 17 days after cell implantation) is shown here. The sites of Adv5-SV-DNE1 and Adv5-SV-LacZ injections are indicated on the mouse flank by D and L, respectively. (B) Changes in tumor size. The procedures and subjects used for experiment are the same as in (A). Each column with a bar represents the mean ± SD of weight (in grams) of tumors resected from each SCID mouse group, comprising 8 tumors in their flanks. Untreated, Adv-LacZ, and Adv-DNE1 represent intratumoral injections with PBS, Adv5-SV-LacZ, and Adv5-SV-DNE1, respectively. A statistically significant difference in tumor weight between the mouse groups is shown by asterisks. (C) Inhibition of tumor induction. Mutu I cells (1×10^7) preexposed to Adv5-SV-DNE1 or Adv5-SV-LacZ (m.o.i. of 2) were implanted subcutaneously in both flanks of each of four SCID mice, and tumor formation was observed. D and L indicate the implantation sites of Adv5-SV-DNE1- and Adv5-SV-LacZ-preexposed cells, respectively. A representative result photographed 14 days after cell implantation is shown.

higher frequency than that of spontaneous isolation (our unpublished data), suggesting that the dnEBNA1 acts effectively not only against the common laboratory strain of EBV such as Akata, but also against other wild strains. Accordingly, the dnEBNA1 may facilitate the rapid *in vitro* production of an isogenic pair of EBV-positive and -negative cell clones from a variety of EBV tumor lines. Since an isogenic system has been reported for only a few BL lines, with low frequency [11,16,43], such analytical subjects would benefit the progress of studies on EBV oncogenicity.

Concomitant with eradication of EBV, our dnEBNA1 inhibited the growth of the naturally occurring EBV-positive BL tumor cells *in vitro* and *in vivo*. Interestingly, this growth impairment was already evident *in vitro* 1 to 2 days after Adv inoculation, whereas EBV loss was usually recognizable 3 days after Adv inoculation. This implies that dnEBNA1 might interfere not only through eradication of viral episomes, but directly via a putative wtEBNA1 function implicated in activating the cell cycle [12,26,30], although this has yet to be confirmed [14,16,17,44]. Similar studies on tumor cells that have integrated EBV genomes will be necessary to test this possibility. A recent study by others utilizing similar EBNA1 mutants has suggested that EBV, and wtEBNA1 itself in particular, was involved in the survival/persistence *in vitro* and *in vivo* of virus-infected cells [45]. In the article, an apoptotic event was induced in some but not all cells expressing dnEBNA1. Consistent with the result, our data (unpublished) also showed that only a minor fraction (~ 25%) of dnEBNA1-delivered Akata-EC BL cells entered into early apoptosis, assessed by annexin V expression, before EBV genomes were eradicated, though this is not the case with Mutu I BL cells. These findings suggested again that dnEBNA1 would check the cell survival/growth, at least in BL cells, through apoptosis and another undefined mechanism(s) [45]. We are now further assessing the inhibitory effects of dnEBNA1 on the growth of various cell types, including EBV-carrying T or NK cells established spontaneously from lethal EBV-induced lymphoproliferative diseases [3,46].

Although the precise molecular mechanism by which our dnEBNA1 eliminates EBV from cells is not yet fully understood, several mechanisms are feasible based on the domain structure. The DNA binding/dimerization domain enables the dnEBNA1 molecules to dimerize, thereby competing against wtEBNA1 homodimers (functional form) for occupancy on the specific *cis*-acting element in *ori*P. In addition, dnEBNA1 could conceivably heterodimerize with wtEBNA1, as described in a recent report using a similar mutant [44]. This could result in a decrease in wtEBNA1 homodimers by depriving them of dimerization partners. The dnEBNA1–wtEBNA1 heterodimers (nonfunctional form) would also preclude binding of wtEBNA1 homodimers to *ori*P. In either case, dnEBNA1 is deemed to inhibit directly viral episome maintenance mediated by the interaction of the wtEBNA1 homodimer with *ori*P. Moreover, the inhibitory effects of dnEBNA1 against wtEBNA1 binding to *ori*P may abolish the enhancer activity of *ori*P for Cp and Wp, which decelerates wtEBNA1 mRNA transcription (and probably other EBNAs and LMP1/2B) in cells of Latency III [19,22,24,32,33,44]. Down regulation of wtEBNA1 synthesis would also occur in cells of Latency I or II because Qp-driven wtEBNA1 transcription is autorepressed via wtEBNA1 binding to negative regulatory elements for Qp (NRE-Qp) [25]. If dnEBNA1 homodimers

and/or dnEBNA1–wtEBNA1 heterodimers exist in abundance, they would bind to NRE-Qp, thus leading to down regulation of Qp activity. Such suppressive effects of dnEBNA1 on *de novo* wtEBNA1 synthesis via mediation of promoter regulation may also play an indirect role in inhibiting viral episome maintenance. Further investigation into this proposal is now being undertaken.

The molecular balance between dnEBNA1 and wtEBNA1 appears to be a critical factor in achieving efficient dominant-negative effects. This was seen here in the EBER1-ISH experiments, which showed that EBV-lost clones varied significantly, even in the same cell line, according to whether the introduced dnEBNA1 gene was driven by SVp or CMVp. For example, when NU-GC-3/rEBV cells were inoculated with Adv5-SV-DNE1 or with Adv5-CV-DNE1, at the same m.o.i. of 20, the incidence of EBER1-negative cells was significantly different: 69.3 ± 6.2% for SVp vs 88.6 ± 3.1% for CMVp ($P < 0.01$ by t test) 9 days postinoculation. The data indicate that there may be a minimum threshold of the stoichiometric dnEBNA1:wtEBNA1 ratio that can make the effects of dnEBNA1 overt, although this was not determined in the present study.

An epidemiological study estimates the annual incidence of EBV-associated human tumors worldwide to be approximately 500,000 [47]. These EBV-associated diseases are often uncontrollable by currently available treatments. A promising therapeutic approach against these diseases is adoptive immune transfer of EBV-specific cytotoxic T lymphocytes (CTL) [48,49], although several problems remain [50]. An alternative approach, based on evidence that the EBV genome, or the specific gene, is virtually implicated in the cellular acquisition of malignant phenotypes [1,7–18,43], involves single EBV gene- or EBV genome (machinery)-targeted remedial strategies, some of which are considered to have potential as treatments [51–55]. However, most EBV latent genes, other than EBNA1, are silenced in tumor cells [1,2,4,5,39,40,42,46] or are heterogeneously expressed, even in individual tumors [56–58], thus limiting clinical approaches that target these viral latent genes. Because of its wide applicability and selectivity, EBNA1-based or -targeted molecular therapy would be more suitable for clinical application [52,55,59].

Rigorous investigations have defined the CTL epitope-clustered location in EBNA1 as the C-terminal, DNA-binding/dimerization domain [60,61]. However, EBNA1-specific $CD8^+$ CTL do not efficiently recognize target cells expressing the full-length EBNA1 protein [60]. This is due in part to the Gly_2-Ala repeat domain, which inhibits MHC class I-restricted presentation of the epitopes of EBNA1 [62]. Our dnEBNA1 lacks the Gly_2-Ala repeat domain, but still has the C-terminal, CTL epitope-rich region. This knowledge raises some concerns about the therapeutic use of dnEBNA1, for although transduction of dnEBNA1 may favorably potentiate EBNA1-specific CTL recognition of virus-infected tumor cells, it may also expose normal cells to CTL. To avoid such disadvantages, tumor-specific transduction and/or expression of dnEBNA1 or intentional conservation of the Gly_2-Ala repeats (preferably as a functionally minimal form) within the dnEBNA1 structure would be necessary.

Materials and Methods

Cell lines. EBV-converted or -reinfected cell lines were established by infecting virus-negative cells with rEBV (Akata strain), which carries the *neo*^{r} as a selective marker [38]. In this study, each rEBV-positive line was denoted by the name of the EBV-negative parental cell line followed by "/rEBV" (Table 1), i.e., Akata$^-$/rEBV [14], MT-2/rEBV [40], NU-GC-3/rEBV [15,39], and BJAB/rEBV [41]. Converted cell lines were maintained in RPMI 1640 culture medium containing 10% fetal calf serum and G418 (Sigma–Aldrich, Tokyo, Japan) at appropriate concentrations (0.5–1 mg/ml) for selection. In some experiments, G418 was removed from cultures during an observation period. Southern blot hybridization confirmed that all the converted cell lines harbored the rEBV genome in an episomal, not integrated, form (data not shown). Mutu I [42] (clone 79, kindly provided by Dr. J. Sample, St. Jude Children's Research Hospital, Memphis, TN, USA) and Akata-EC (early-cultured Akata) [17] were used as test cells of naturally EBV-infected BL cell lines. Hygromycin B (Wako Pure Chemical Industries, Ltd., Osaka, Japan) was used to grow cells selectively in dual gene transduction experiments (see below). The MRC-5 cell line was purchased from the American Type Culture Collection (Rockville, MD, USA). 293/DNE1 is a hygromycin-selected 293 cell clone that stably expresses the mtEBNA1 protein.

Plasmid construction. The mtEBNA1 structure was made according to the EBNA1 sequence of B95-8 EBV [63]. The mtEBNA1 consists of the following functional domains of wtEBNA1 (641 amino acids of the B95-8 strain): the nuclear localization signal (NLS; aa 379 to 386) and the C-terminal region spanning the DNA linking/dimerization domain to the acidic tail (aa 451 to 641) (Fig. 1) [22,32–34]. Briefly, a coding segment of the partial NLS (aa 382 to 386) connected to the C-terminal domain region (aa 451 to 641) was amplified by PCR using a cloned *Bam*HI-K of B95-8 EBV (pUC119-B95BamK) as the template. The mutagenized nucleotides ATC were introduced into the forward chimeric junction primer, in place of GAG in the native NLS (genomic coordinates 96807 to 96809 according to the new version of the B95-8 EBV sequence databases, GenBank Accession No. AJ507799), thereby generating a *Bgl*II recognition site useful for the next DNA recombination without amino acid substitution (relating to codons Arg^{382} and Ser^{383}). The reverse adaptor primer contained the artificial *Bal*I and *Eco*RI recognition sites (necessary for cloning) followed by sequences encompassing the 3′end of the acidic tail domain. An amplified product was cloned into the *Bgl*II–*Eco*RI site of the pIRES2-EGFP vector (BD Bioscience Clontech, Tokyo, Japan), resulting in pIRES2-EGFP/Bg-EI-ΔDNE1. A synthesized oligomer adaptor was then prepared, composed of coding sequences for the N-terminal part of mtEBNA1 (Met^1-Lys^{379}-Arg^{380}-Pro^{381}) with *Nhe*I- and *Bgl*II-compatible sites at its 5′and 3′ends, respectively. The adaptor was inserted into *Nhe*I–*Bgl*II site of pIRES2-EGFP/Bg-EI-ΔDNE1, yielding pIRES2-EGFP/DNE1. A 0.6-kb *Eco*RI fragment of pIRES2-EGFP/DNE1, corresponding to the expected entire structure of mtEBNA1, was cloned into SVp-driven vector, pSG5-neo, a modified pSG5 (Stratagene, La Jolla, CA, USA) into which the *neo*^{r} cassette had been inserted. The same 0.6-kb *Eco*RI fragment was cloned also into the CMVp-driven vector pcDNA3 (Invitrogen, Groningen, Netherlands), resulting in pSG5-neo/DNE1 and pcDNA3-DNE1, respectively. A wtEBNA1 expression plasmid, pSG5m-neo/AKE1, was constructed by ligating a 2.1-kb *Xho*II–*Bal*I fragment from a cloned *Bam*HI-K of Akata EBV strain [37] into the *Bam*HI–*Sma*I site of pSG5m-neo (pSG5-neo with additional cloning sites). Expression plasmids for EGFP (derived from pIRES2-EGFP) and *Escherichia coli* β-galactosidase (LacZ; derived from pSV-β-Gal; Promega, Madison, WI, USA) were also cloned into pSG5m-neo and pcDNA3.

doi:10.1016/j.ymthe.2004.12.017

Plasmids for IRES-mediated bicistronic expression of the mtEBNA1 gene and the *hyg*^{r} gene, as a positive selection marker, were also constructed for mtEBNA1-transduced cell sorting experiments (Fig. 4C). Briefly, the *hyg*^{r}–poly(A) segment of pCEP4 (Invitrogen) was PCR-amplified with primers to create *Eco*RV and *Xho*I recognition sequences at the 5′ and 3′ ends, respectively, and cloned into pBluescript II SK(−) (Stratagene), resulting in pBKN-HYG-pA. The *Eco*T22I (blunted)–*Bst*XI fragment from pIRES2-EGFP/DNE1, which contains CMVp-DNE1-IRES, was inserted into the *Sac*I (blunted)–*Bst*XI site of pBKN-HYG-pA, yielding the plasmid pCMV-DIH containing CMVp-DNE1-IRES-*hyg*^{r}-polyA. A plasmid containing SV40p-DNE1-IRES-*hyg*^{r}-polyA, pSG5-DIH, was also made by replacing CMVp of pCMV-DIH with SV40p. Plasmids for coexpression of lacZ and *hyg*^{r} (pCMV-LIH and pSG5-LIH) were constructed as controls.

The expression units of the plasmids described above (details will be provided upon request) were incorporated into Adv's as explained below.

Isolation and purification of Adv. All Adv's used in this study were developed using the *in vitro* ligation method [35]. Adenovirus genome plasmids, termed pAdHM4 [35] and pAdHM36 [36], were used to construct the standard E1/E3-deleted Adv5 and its fiber-replaced variant (Adv5/35f), respectively. Prepared recombinant Adv genome plasmids were linearized with *Pac*I (New England Biolabs, Inc., Beverly, MA, USA) and then transfected into 293 cells. After plaque purification, Adv isolates were checked for the restriction pattern of viral DNA and expression of incorporated genes. Confirmed virus clones were expanded and purified by sequential ultracentrifugation, using CsCl step gradients, followed by dialysis [64]. Purified virus was aliquoted into small volumes and stored at −80°C until use. Titers of virus stock were determined by the standard plaque-forming end-point assay [64].

In this study, both SVp-driven and CMVp-driven expression units were constructed for each gene, e.g., pSG5-neo/DNE1 and pcDNA3-DNE1 (see above), and incorporated individually into Adv5 and Adv5/35f. Of the four kinds of Adv per gene, the most suitable was preliminarily selected for each cell line in terms of the highest gene transfer efficiency (Adv5 or Adv5/35f) and gene expression levels (SVp or CMVp). Adv's were designated "Adv type-driving promoter-incorporated gene." For example, Adv5 for SVp-driven mtEBNA1 and Adv5/35f for CMVp-driven LacZ were referred to as Adv5-SV-DNE1 and Adv5/35f-CV-LacZ, respectively. Adv's for IRES-mediated coexpression of mtEBNA1 (or LacZ) and *hyg*^{r} were referred to as Adv5 (or Adv5/35f)-SV (or CV)-DIH (or LIH) (Fig. 4C).

Adv infection and flow cytometric analysis. Susceptibility of cell lines to Adv infection was examined by exposing cells to Adv5 (or Adv5/35f)-SV (or CV)-EGFP at various m.o.i. for 2 h at 37°C. After cultivation for 3 days, EGFP-positive cells were measured by flow cytometry (FACScan Cytometer, BD Bioscience Clontech) and compared with cells inoculated with each corresponding Adv type for LacZ expression at the same m.o.i. and with mock-inoculated cells as controls. Immediately before analysis, cells were stained with 2 μM 7-amino-actinomycin D (Sigma–Aldrich) to exclude nonviable cells.

Selection of Adv-infected cells. Cells that had been successfully infected with Adv5-SV (or CV)-DIH (or LIH) were sorted from uninfected cells by hygromycin B-based positive selection (Fig. 4D). The optimal conditions for this short-term drug pulse were determined preliminarily for each cell line by strictly comparing Adv-DIH-inoculated cultures with Adv-LIH-inoculated cultures (selection procedures following Adv inoculation for Mutu I cells, as an example, are described under Results and in the legend to Fig. 4D). The resultant surviving cells after drug selection were then evaluated for EBV genome carriage (e.g., by *in situ* hybridization, see below). Using immunoblot analysis, it was confirmed that Adv5-SV (or CV)-DIH (or LIH) achieved the same levels of mtEBNA1 and LacZ protein expression as Adv5-SV (or CV)-DNE1 (or LacZ) did (data not shown).

Quantitative PCR. The EBV genome was quantified by real-time PCR with the LightCycler system (Roche Diagnostics, Mannheim, Germany) using primers directed for a region within the LMP1 gene. The sequences were LMP1-Pv4S, 5′-GTTGATCTCCTTTGGCTCCTC-3′ (genome coordinates 168358–168338, according to the new databases mentioned above), and LMP1-Pv4AS, 5′-GTGTCTGCCCTCGTTGG-3′ (168191–168207). Two specific hybridization probes were used: LMP1-v4PR/FL, 5′-TGATGAACAC-CACCACGATGACTCC-[fluorescein]-3′ (168287–168263), and LMP1-v4PR/LC, 5′-[LC-Red640]-TCCCGCACCCTCAACAAGCTAC-PO_4-3′ (168261–168240) (synthesized by Nihon Gene Research Labs, Inc., Sendai, Japan). Template DNA was extracted with a FlexiGene DNA Kit (Qiagen, Tokyo, Japan), treated with 20 μl of RNase A (10 μg/ml, type IA; Sigma–Aldrich), and predigested with *Eco*RI to minimize the viscosity of DNA solutions, thereby ensuring accuracy in the amount of DNA dispensed into capillaries. The reaction mixture was 20 μl in volume and consisted of 10 pmol of each primer, 4 pmol of each probe, 10 μl of QuantiTect Probe PCR Kit Master Mix (Qiagen), and 5 μl of the predigested DNA (50 ng) per reaction. The cycling protocol was as follows: preincubation at 94°C for 15 min followed by 40 cycles of denaturation at 94°C for 15 s, annealing at 60°C for 20 s, and extension at 72°C for 20 s. Data were gained according to the settings recommended by the manufacturer and analyzed with LightCycler software version 3.5. Serial 10-fold dilutions of a plasmid amplicon containing the LMP1 target sequence (2×10^4 to 2×10^1 copies per capillary) were used to generate a standard plot for calculation of EBV genome number. To calibrate the data and to check the integrity of DNA samples, the β-globin gene was quantified in parallel (information about primers/probes can be provided upon request). The Namalwa cell line [65], which carries two EBV genomes per cell, was used as a positive control for each LightCycler assay to check reproducibility.

Immunoblot. The basic immunoblot procedures used have been described previously [46]. EBNA1 expression was examined with reference human serum (anti-EBNA1 titer, 1:1280) or EBNA1-monospecific rabbit immune serum (kindly provided by Dr. T. Tsurumi, Aichi Cancer Center, Nagoya, Japan) as the primary antibody. Protein bands were detected using the enhanced chemiluminescence system (Amersham Pharmacia). In some experiments, specific chemiluminescent signals were scanned by the ATTO LightCapture System Cool Saver software (Type AE-6962; ATTO Co. Ltd., Tokyo, Japan) and intensity was analyzed with a CS analyzer (ATTO). To evaluate the relative levels of wtEBNA1 protein expression, scanned values specific for wtEBNA1 were normalized to those of β-actin signals of the same samples probed with the AC-15 monoclonal antibody (Sigma–Aldrich) as an internal control.

Cell proliferation assay. Viable cell kinetics were assessed by trypan blue dye exclusion or by production of water-soluble formazan in the sulfonated tetrazolium salt (WST-1) assay (Takara Biotech, Tokyo, Japan). The WST-1 assay was done in triplicate in 96-well plates, and an absorbance of 450 nm (A_{450}) was determined for each well, followed by subtracting the background absorbance (A_{600}) from each A_{450} measurement.

In situ hybridization. To detect EBV genome-harboring cells, FISH was carried out according to the method reported previously [66]. Briefly, the cosmid pJB8, containing an *Eco*RI-A fragment (37 kb) of EBV DNA, was used to make a probe labeled with biotin-16–dUTP (Roche Diagnostics) by nick translation. Ten microliters of hybridization solution (Sigma–Aldrich) containing 20 ng of biotinylated probe was denatured at 70°C for 2 min and applied to preparations on glass slides, which were then incubated at 37°C overnight in a humidified chamber. The slides were washed twice for 10 min in 50% formamide in 2× standard saline citrate (SSC) (0.3 mM sodium chloride, 30 mM sodium citrate, pH 7.0) at 43°C, followed by two rinses in 2× SSC at 37°C. The hybridized probe was detected by incubation with fluorescein avidin D (Vector Laboratories, Burlingame, CA, USA), according to the procedure described previously [66]. The interphase nuclei were counterstained with propidium iodide (Sigma–Aldrich) and diamino-2-phenylindole (SERVA Feinbiochemica, Heidelberg, Germany). The slides were observed with a BX50 epifluorescence microscope (Olympus, Tokyo, Japan). Hybridization signals were captured with a cooled CCD camera and merged using a computer workstation equipped with the M-FISH system (Photometrics-Seki Technotron, Tokyo, Japan). EBER1-ISH was also carried out to assess the EBV persistence or loss in rEBV-converted cells, as previously described in detail [46].

Animal experiments. All animal experiments were conducted according to the guidelines of the Animal Experiment Committee of Kochi Medical School. The therapeutic potential of mtEBNA1 was assessed by its ability to inhibit tumor growth/induction *in vivo* using a xenograft animal model. Mutu I BL cells (1×10^7) suspended in 200 μl of PBS, pH 7.2, were implanted subcutaneously in both hind flanks of 6- to 8-week-old SCID mice (female, FOX CHASE C.B-17/Icr-scid Jcl; CLEA, Tokyo, Japan). Twelve mice (i.e., 24 flanks) were used for this experiment. Once tumors had become unequivocally palpable (0.4–0.5 cm in diameter), mice received intratumoral injection of either Adv5-SV-DNE1 or Adv5-SV-LacZ as the control (10^8 pfu per dose) into each flank. Some mice received an injection of PBS in place of Adv5-SV-LacZ as a mock injection control. Adv5-SV-DNE1, Adv5-SV-LacZ, and PBS were injected into eight tumors each. In an additional experiment, Mutu I cells were preexposed to Adv5-SV-DNE1 or Adv5-SV-LacZ and on the next day 1×10^7 viable cells were likewise implanted in each flank of SCID mice (4 mice were tested). All mice were monitored for tumor growth/induction for up to 4 weeks after cell implantation and photographed and euthanized if the tumor exceeded 2 cm in dimension or the mouse was apparently ill. The resected tumors were weighed, and some of the tissues were examined histologically and screened for EBV.

Statistical analysis. Data of wtEBNA1 protein levels and cell growth kinetics were expressed as the relative ratio (or percentage) of scanned (or absorbance) values in cells inoculated with Adv's against those of mock-inoculated cells. The statistical method used was mainly two-way analysis of variance. In analyses of the effects of Adv's, the factors consisted of time after Adv inoculation and Adv type (Adv-DNE1 and Adv-LacZ) used, followed by the post hoc Tukey or Dunnett test. The *t* test and the Mann–Whitney *U* test were also used for some results. *P* values less than 0.05 were considered statistically significant.

ACKNOWLEDGMENTS

We thank Mrs. Kazuyo Ito for help with manuscript preparation. We also thank Dr. Taketoshi Taniguchi for kindly providing plasmids. This work was supported in part by research grants from the Japanese Ministry of Education, Culture, Sports, and Science (12213095 and 15590421 (S.I.), 13770152 (M.K.), 14570750 (H.W.); by a grant for Child Health and Development (16C-1 (S.I.)) from the Japanese Ministry of Health, Labor, and Welfare; by the Sagawa Cancer Research Foundation (S.I.), Kyoto; and by the President Research Fund of Kochi Medical School Hospital (S.I.), Kochi, Japan.

RECEIVED FOR PUBLICATION NOVEMBER 30, 2003; ACCEPTED DECEMBER 18, 2004.

APPENDIX A. SUPPLEMENTARY DATA

Supplementary data associated with this article can be found, in the online version, at doi: 10.1016/j.ymthe.2004.12.017.

REFERENCES

1. Rickinson, A. B., and Kieff, E. (2001). Epstein–Barr virus. In *Fields Virology* (D. M. Knipe, P. M. Howley Eds.), 4th ed., Vol. 2, pp. 2575–2627. Lippincott, Philadelphia.
2. Pallesen, G., Hamilton-Dutoit, S. J., Rowe, M., and Young, L. S. (1991). Expression of Epstein–Barr virus latent gene products in tumour cells of Hodgkin's disease. *Lancet* **337:** 320–322.
3. Harabuchi, Y., *et al.* (1990). Epstein–Barr virus in nasal T-cell lymphomas in patients with lethal midline granuloma. *Lancet* **335:** 128–130.
4. Imai, S., *et al.* (1994). Gastric carcinoma: monoclonal epithelial malignant cells expressing Epstein–Barr virus latent infection protein. *Proc. Natl. Acad. Sci. USA* **91:** 9131–9135.
5. Sugiura, M., *et al.* (1996). Transcriptional analysis of Epstein–Barr virus gene expression in EBV-positive gastric carcinoma: unique viral latency in the tumour cells. *Br. J. Cancer* **74:** 625–631.
6. Jaffe, E. S., *et al.* (1996). Report of the Workshop on Nasal and Related Extranodal Angiocentric T/Natural Killer Cell Lymphomas: definitions, differential diagnosis, and epidemiology. *Am. J. Surg. Pathol.* **20:** 103–111.
7. Kieff, E., and Rickinson, A. B. (2001). Epstein–Barr virus and its replication. In *Fields Virology* (D. M. Knipe, P. M. Howley Eds.), 4th ed., Vol. 2, pp. 2511–2573. Lippincott, Philadelphia.
8. Griffin, B. E., and Karran, L. (1984). Immortalization of monkey epithelial cells by specific fragments of Epstein–Barr virus DNA. *Nature* **309:** 78–82.
9. Hammerschmidt, W., and Sugden, B. (1989). Genetic analysis of immortalizing functions of Epstein–Barr virus in human B lymphocytes. *Nature* **340:** 393–397.
10. Wei, M. X., and Ooka, T. (1989). A transforming function of the BARF1 gene encoded by Epstein–Barr virus. *EMBO J.* **8:** 2897–2903.
11. Shimizu, N., Tanabe-Tochikura, A., Kuroiwa, Y., and Takada, K. (1994). Isolation of Epstein–Barr virus (EBV)-negative cell clones from the EBV-positive Burkitt's lymphoma (BL) line Akata: malignant phenotypes of BL cells are dependent on EBV. *J. Virol.* **68:** 6069–6073.
12. Wilson, J. B., Bell, J. L., and Levine, A. J. (1996). Expression of Epstein–Barr virus nuclear antigen-1 induces B cell neoplasia in transgenic mice. *EMBO J.* **15:** 3117–3126.
13. Kulwichit, W., Edwards, R. H., Davenport, E. M., Baskar, J. F., Godfrey, V., and Raab-Traub, N. (1998). Expression of the Epstein–Barr virus latent membrane protein 1 induces B cell lymphoma in transgenic mice. *Proc. Natl. Acad. Sci. USA* **95:** 11963–11968.
14. Komano, J., Maruo, S., Kurozumi, K., Oda, T., and Takada, K. (1999). Oncogenic role of Epstein–Barr virus-encoded RNAs in Burkitt's lymphoma cell line Akata. *J. Virol.* **73:** 9827–9831.
15. Nishikawa, J., Imai, S., Oda, T., Kojima, T., Okita, K., and Takada, K. (1999). Epstein–Barr virus promotes epithelial cell growth in the absence of EBNA2 and LMP1 expression. *J. Virol.* **73:** 1286–1292.
16. Kitagawa, N., *et al.* (2000). Epstein–Barr virus-encoded poly(A)$^-$ RNA supports Burkitt's lymphoma growth through interleukin-10 induction. *EMBO J.* **19:** 6742–6750.
17. Maruo, S., Nanbo, A., and Takada, K. (2001). Replacement of the Epstein–Barr virus plasmid with the EBER plasmid in Burkitt's lymphoma cells. *J. Virol.* **75:** 9977–9982.
18. Imai, S., Nishikawa, J., Kuroda, M., and Takada, K. (2001). Epstein–Barr virus infection of human epithelial cells. *Curr. Top. Microbiol. Immunol.* **258:** 161–184.
19. Rogers, R. P., Woisetschlaeger, M., and Speck, S. H. (1990). Alternative splicing dictates translational start in Epstein–Barr virus transcripts. *EMBO J.* **9:** 2273–2277.
20. Schaefer, B. C., Strominger, J. L., and Speck, S. H. (1995). Redefining the Epstein–Barr virus-encoded nuclear antigen EBNA-1 gene promoter and transcription initiation site in group I Burkitt lymphoma cell lines. *Proc. Natl. Acad. Sci. USA* **92:** 10565–10569.
21. Yates, J. L., Warren, N., and Sugden, B. (1985). Stable replication of plasmids derived from Epstein–Barr virus in various mammalian cells. *Nature* **313:** 812–815.
22. Leight, E. R., and Sugden, B. (2000). EBNA-1: a protein pivotal to latent infection by Epstein–Barr virus. *Rev. Med. Virol.* **10:** 83–100.
23. Gahn, T. A., and Sugden, B. (1995). An EBNA-1-dependent enhancer acts from a distance of 10 kilobase pairs to increase expression of the Epstein–Barr virus LMP gene. *J. Virol.* **69:** 2633–2636.
24. Puglielli, M. T., Woisetschlaeger, M., and Speck, S. H. (1996). OriP is essential for EBNA gene promoter activity in Epstein–Barr virus-immortalized lymphoblastoid cell lines. *J. Virol.* **70:** 5758–5768.
25. Sample, J., Henson, E. B., and Sample, C. (1992). The Epstein–Barr virus nuclear protein 1 promoter active in type I latency is autoregulated. *J. Virol.* **66:** 4654–4661.
26. Snudden, D. K., Hearing, J., Smith, P. R., Grasser, F. A., and Griffin, B. E. (1994). EBNA-1, the major nuclear antigen of Epstein–Barr virus, resembles 'RGG' RNA binding proteins. *EMBO J.* **13:** 4840–4847.
27. Srinivas, S. K., and Sixbey, J. W. (1995). Epstein–Barr virus induction of recombinase-activating genes RAG1 and RAG2. *J. Virol.* **69:** 8155–8158.
28. Kube, D., *et al.* (1999). Expression of Epstein–Barr virus nuclear antigen 1 is associated with enhanced expression of CD25 in the Hodgkin cell line L428. *J. Virol.* **73:** 1630–1636.
29. Sugawara, Y., Makuuchi, M., Kato, N., Shimotohno, K., and Takada, K. (2000). Enhancement of hepatitis C virus replication by Epstein–Barr virus-encoded nuclear antigen 1. *EMBO J.* **18:** 5755–5760.
30. Holowaty, M. N., *et al.* (2003). Protein profiling with Epstein–Barr nuclear antigen-1 reveals an interaction with the herpesvirus-associated ubiquitin-specific protease HAUSP/USP7. *J. Biol. Chem.* **278:** 29987–29994.
31. Steigerwald-Mullen, P., Kurilla, M. G., and Braciale, T. J. (2000). Type 2 cytokines predominate in the human CD4(+) T-lymphocyte response to Epstein–Barr virus nuclear antigen 1. *J. Virol.* **74:** 6748–6759.
32. Ceccarelli, D. F., and Frappier, L. (2000). Functional analyses of the EBNA1 origin DNA binding protein of Epstein–Barr virus. *J. Virol.* **74:** 4939–4948.
33. Wu, H., Kapoor, P., and Frappier, L. (2002). Separation of the DNA replication, segregation, and transcriptional activation functions of Epstein–Barr nuclear antigen 1. *J. Virol.* **76:** 2480–2490.
34. Kirchmaier, A. L., and Sugden, B. (1997). Dominant-negative inhibitors of EBNA-1 of Epstein–Barr virus. *J. Virol.* **71:** 1766–1775.
35. Mizuguchi, H., and Kay, M. A. (1998). Efficient construction of a recombinant adenovirus vector by an improved in vitro ligation method. *Hum. Gene Ther.* **9:** 2577–2583.
36. Mizuguchi, H., and Hayakawa, T. (2002). Adenovirus vectors containing chimeric type 5 and type 35 fiber proteins exhibit altered and expanded tropism and increase the size limit of foreign genes. *Gene* **285:** 69–77.
37. Takada, K., *et al.* (1991). An Epstein–Barr virus-producer line Akata: establishment of the cell line and analysis of viral DNA. *Virus Genes* **5:** 147–156.

doi:10.1016/j.ymthe.2004.12.017

38. Shimizu, N., Yoshiyama, H., and Takada, K. (1996). Clonal propagation of Epstein–Barr virus (EBV) recombinants in EBV-negative Akata cells. *J. Virol.* **70:** 7260–7263.
39. Imai, S., Nishikawa, J., and Takada, K. (1998). Cell-to-cell contact as an efficient mode of Epstein–Barr virus infection of diverse human epithelial cells. *J. Virol.* **72:** 4371–4378.
40. Yoshiyama, H., Shimizu, N., and Takada, K. (1995). Persistent Epstein–Barr virus infection in a human T-cell line: unique program of latent virus expression. *EMBO J.* **14:** 3706–3711.
41. Kanamori, M., *et al.* (2004). Epstein–Barr virus nuclear antigen leader protein induces expression of thymus and activation-regulated chemokine in B cells. *J. Virol.* **78:** 3984–3993.
42. Gregory, C. D., Rowe, M., and Rickinson, A. B. (1990). Different Epstein–Barr virus–B cell interactions in phenotypically distinct clones of a Burkitt's lymphoma cell line. *J. Gen. Virol.* **71:** 1481–1495.
43. Chodosh, J., Holder, V. P., Gan, Y. J., Belgaumi, A., Sample, J., and Sixbey, J. W. (1998). Eradication of latent Epstein–Barr virus by hydroxyurea alters the growth-transformed cell phenotype. *J. Infect. Dis.* **177:** 1194–1201.
44. Kang, M. S., Hung, S. C., and Kieff, E. (2001). Epstein–Barr virus nuclear antigen 1 activates transcription from episomal but not integrated DNA and does not alter lymphocyte growth. *Proc. Natl. Acad. Sci. USA* **98:** 15233–15238.
45. Kennedy, G., Komano, J., and Sugden, B. (2003). Epstein–Barr virus provides a survival factor to Burkitt's lymphomas. *Proc. Natl. Acad. Sci. USA* **100:** 14269–14274.
46. Imai, S., *et al.* (1996). Epstein–Barr virus (EBV)-carrying and -expressing T-cell lines established from severe chronic active EBV infection. *Blood* **87:** 1446–1457.
47. Levin, L. I., and Levine, P. H. (1998). The epidemiology of Epstein–Barr virus-associated human cancer. *Gann Monogr. Cancer Res.* **45:** 51–74.
48. Heslop, H. E., *et al.* (1996). Long-term restoration of immunity against Epstein–Barr virus infection by adoptive transfer of gene-modified virus-specific T lymphocytes. *Nat. Med.* **2:** 551–555.
49. Gottschalk, S., *et al.* (2003). Generating CTLs against the subdominant Epstein–Barr virus LMP1 antigen for the adoptive immunotherapy of EBV-associated malignancies. *Blood* **101:** 1905–1912.
50. Gottschalk, S., *et al.* (2001). An Epstein–Barr virus deletion mutant associated with fatal lymphoproliferative disease unresponsive to therapy with virus-specific CTLs. *Blood* **97:** 835–843.
51. Banerjee, S., Livanos, E., and Vos, J. M. H. (1995). Therapeutic gene delivery in human B-lymphoblastoid cells by engineered non-transforming infectious Epstein–Barr virus. *Nat. Med.* **1:** 1303–1308.
52. Judde, J. G., Spangler, G., Magrath, I., and Bhatia, K. (1996). Use of Epstein–Barr virus nuclear antigen-1 in targeted therapy of EBV-associated neoplasia. *Hum. Gene Ther.* **7:** 647–653.
53. Franken, M., Estabrooks, A., Cavacini, L., Sherburne, B., Wang, F., and Scadden, D. T. (1996). Epstein–Barr virus-driven gene therapy for EBV-related lymphomas. *Nat. Med.* **2:** 1379–1382.
54. Westphal, E. M., Mauser, A., Swenson, J., Davis, M. G., Talarico, C. L., and Kenney, S. C. (1999). Induction of lytic Epstein–Barr virus (EBV) infection in EBV-associated malignancies using adenovirus vectors in vitro and in vivo. *Cancer Res.* **59:** 1485–1491.
55. Li, J. H., *et al.* (2002). Tumor-targeted gene therapy for nasopharyngeal carcinoma. *Cancer Res.* **62:** 171–178.
56. Niedobitek, G., *et al.* (1995). Heterogeneous expression of Epstein–Barr virus latent proteins in endemic Burkitt's lymphoma. *Blood* **86:** 659–665.
57. Tao, Q., Robertson, K. D., Manns, A., Hildesheim, A., and Ambinder, R. F. (1998). Epstein–Barr virus (EBV) in endemic Burkitt's lymphoma: molecular analysis of primary tumor tissue. *Blood* **91:** 1373–1381.
58. Xue, S. A., *et al.* (2002). Promiscuous expression of Epstein–Barr virus genes in Burkitt's lymphoma from the central African country Malawi. *Int. J. Cancer* **99:** 635–643.
59. Roth, G., Curiel, T., and Lacy, J. (1994). Epstein–Barr viral nuclear antigen 1 antisense oligodeoxynucleotide inhibits proliferation of Epstein–Barr virus-immortalized B cells. *Blood* **84:** 582–587.
60. Blake, N., *et al.* (1997). Human $CD8^+$ T cell responses to EBV EBNA1: HLA class I presentation of the (Gly-Ala)-containing protein requires exogenous processing. *Immunity* **7:** 791–802.
61. Paludan, C., *et al.* (2002). Epstein–Barr nuclear antigen 1-specific CD4(+) Th1 cells kill Burkitt's lymphoma cells. *J. Immunol.* **169:** 1593–1603.
62. Levitskaya, J., Shapiro, A., Leonchiks, A., Ciechanover, A., and Masucci, M. G. (1997). Inhibition of ubiquitin/proteasome-dependent protein degradation by the Gly-Ala repeat domain of the Epstein–Barr virus nuclear antigen 1. *Proc. Natl. Acad. Sci. USA* **94:** 12616–12620.
63. Baer, R., *et al.* (1984). DNA sequence and expression of the B95-8 Epstein–Barr virus genome. *Nature* **310:** 207–211.
64. Kanegae, Y., Makimura, M., and Saito, I. (1994). A simple and efficient method for purification of infectious recombinant adenovirus. *Jpn. J. Med. Sci. Biol.* **47:** 157–166.
65. Prichett, R., Pedersen, M., and Kieff, E. (1976). Complexity of EBV homologous DNA in continuous lymphoblastoid cell lines. *Virology* **74:** 227–231.
66. Taguchi, T., *et al.* (1993). Chromosomal localization of the OX44 (CD53) leukocyte antigen gene in man and rodents. *Cytogenet. Cell Genet.* **64:** 217–221.

Available online at www.sciencedirect.com

SCIENCE DIRECT

Gene 348 (2005) 157–165

GENE
SECTION
FUNCTIONAL GENOMICS

www.elsevier.com/locate/gene

RNA interference of PPARγ using fiber-modified adenovirus vector efficiently suppresses preadipocyte-to-adipocyte differentiation in 3T3-L1 cells

Tetsuji Hosono[a], Hiroyuki Mizuguchi[b,*], Kazufumi Katayama[c], Naoya Koizumi[b,d], Kenji Kawabata[b], Teruhide Yamaguchi[a], Shinsaku Nakagawa[c], Yoshiteru Watanabe[d], Tadanori Mayumi[e], Takao Hayakawa[f]

[a]*Division of Cellular and Gene Therapy Products, National Institute of Health Sciences, Tokyo 158-8501, Japan*
[b]*Project III, National Institute of Health Sciences, Osaka Branch, Fundamental Research Laboratories for Development of Medicine, Asagi 7-6-8, Saito, Ibaraki, Osaka 567-0085, Japan*
[c]*Department of Biopharmaceutics, Graduate School of Pharmaceutical Sciences, Osaka University, Osaka 565-0871, Japan*
[d]*Department of Pharmaceutics and Biopharmaceutics, Showa Pharmaceutical University, Tokyo 194-8543, Japan*
[e]*Faculty of Pharmaceutical Sciences, Kobe Gakuin University, Hyogo 651-2180, Japan*
[f]*National Institute of Health Sciences, Tokyo 158-8501, Japan*

Received 12 October 2004; received in revised form 14 December 2004; accepted 6 January 2005

Received by T. Sekiya

Abstract

The peroxisome proliferator-activated receptor (PPAR) γ is regarded as a "master regulator" of adipocyte differentiation and is abundantly expressed in adipose. To understand the biological role of PPARγ in adipose, RNA interference (RNAi) of PPARγ should be a powerful tool. 3T3-L1 cell line serves an excellent model to investigate the mechanism of preadipocyte-to-adipocyte differentiation. However, this cell line is difficult to transfect by plasmid vectors and viral vectors. We optimized the transduction of both 3T3-L1 preadipocytes and adipocytes by means of fiber-modified adenovirus (Ad) vectors. Among the various vectors tested, polylysine modification of the C-terminal of the fiber knob most markedly improved the transduction efficiency in both 3T3-L1 preadipocytes and adipocytes. Then, we examined whether fiber-modified Ad vectors with polylysine peptides expressing the small interfering RNA (siRNA) for PPARγ inhibit the differentiation of 3T3-L1 preadipocytes into adipocytes. Oil red O staining and measurement of glycerol-3-phosphate dehydrogenase (GPDH) activity indicated that the vectors effectively suppressed the differentiation of 3T3-L1 preadipocytes to adipocytes. These results suggested that the combination of fiber-modified Ad vectors containing polylysine peptides and RNAi is an effective tool for the study of the biological and physiological mechanism of adipogenesis in adiposity and diabetes using 3T3-L1 models. Ad vector-mediated RNAi for PPARγ should also be useful to clarify the biological role of the PPARγ pathway in various tissues in addition to adipose and for therapeutic application to a variety of diseases, including adiposity and diabetes.

Keywords: Adenovirus vector; PPARγ; RNA interference; Adipocyte

1. Introduction

An understanding of the biological and physiological mechanism of adipogenesis is essential for an improved understanding of adiposity and diabetes. The expression of many transcription factors and adipocyte-specific genes, including CCAAT enhancer binding proteins (C/EBP) and

Abbreviations: CAR, coxsackievirus and adenovirus receptor; GAPDH, glyceraldehyde-3-phosphate dehydrogenase; GPDH, glycerol-3-phosphate dehydrogenase; LacZ, β-galactosidase; PPARγ, peroxisome proliferator-activated receptor γ; RT-PCR, reverse transcription–polymerase chain reaction; shRNA, short hairpin RNA; siRNA, small interfering RNA.

* Corresponding author. Tel.: +81 72 641 9815; fax: +81 72 641 9816.
E-mail address: mizuguch@nihs.go.jp (H. Mizuguchi).

0378-1119/$ - see front matter © 2005 Elsevier B.V. All rights reserved.
doi:10.1016/j.gene.2005.01.005

adipocyte differentiation and determination factor 1/sterol regulatory element binding protein 1 (ADD-1/SREBP-1), is programmatically regulated in the process of adipogenesis (Gregoire et al., 1998; Ntambi and Young-Cheul, 2000). Among them, the peroxisome proliferator-activated receptor (PPAR) γ is regarded as a "master regulator" of adipocyte differentiation and is abundantly expressed in adipose (Tontonoz et al., 1994a,b; Vidal-Puig et al., 1997; Wu et al., 1998; Kubota et al., 1999; Berger and Moller, 2002). PPARγ is a member of the nuclear receptor superfamily and induces transcriptional activation by heterodimerization with the retinoic acid-like receptor (RXR) (Tontonoz et al., 1994a; Berger and Moller, 2002).

Adipocytes are thought to be derived from mesenchymal stem cells, and cell culture models using preadipocyte 3T3-L1 cell lines are extensively used to study preadipocyte-to-adipocyte differentiation (Ntambi and Young-Cheul, 2000). Treatment of 3T3-L1 adipocytes with agonists for PPARγ including thiazolidinediones (TZD), potent insulin sensitizing agents, induces preadipocyte-to-adipocyte differentiation. To understand the factors and mechanisms involved in the process of adipogenesis, studies of loss of function via knock-out/knock-down of target gene expression or gain of function via overexpression are among the most powerful methods. 3T3-L1 cells, however, are not efficiently transfectable. Viral vector-mediated transduction might improve their efficiency.

Among the viral vectors, adenovirus (Ad) vectors have been extensively used to deliver foreign genes to a variety of cell types and tissues both in vitro and in vivo. They can be easily grown to high titer and can efficiently transfer genes into both dividing and non-dividing cells. The efficiency of Ad vector-mediated transduction into 3T3-L1 cells, however, is quite low due to the scarcity of the primary receptor, the coxsackievirus and adenovirus receptor (CAR) (Orlicky et al., 2001). To overcome CAR-dependent transduction, fiber-modified Ad vectors have been developed (Krasnykh et al., 1996; Wickham et al., 1997; Dmitriev et al., 1998; Shayakhmetov et al., 2000; Havenga et al., 2001; Mizuguchi et al., 2001; Mizuguchi and Hayakawa, 2002; Koizumi et al., 2003), containing RGD peptides in the HI loop of the fiber knob, polylysine peptides in the C-terminal end of the fiber knob, or fiber proteins derived from subgroup B Ads such as Ad type 3, -11, or -35. These vectors are infected via αv integrin, heparan sulfates, or CD46 (or CD80 or CD86) on the cellular surface, respectively (Wickham et al., 1997; Dmitriev et al., 1998; Mizuguchi et al., 2001; Gaggar et al., 2003; Segerman et al., 2003; Short et al., 2004).

For studies of loss of function via knockdown of target gene expression, RNA interference (RNAi) has been shown to have great promise for both basic research and therapeutic use. RNAi mediates the sequence-specific suppression of gene expression in a wide variety of eukaryotes by double-stranded RNA homologies to the target gene (McManus and Sharp, 2002). In mammalian cells, small interfering RNA (siRNA), a 19- to 29-nt RNA, leads to the inhibition of target gene expression in a sequence-specific manner (Elbashir et al., 2001). Vector-based siRNA systems, including Ad vectors, have also been developed using RNA polymerase III promoters, such as the U6 promoter or the H1 promoter, to express siRNA (Brummelkamp et al., 2002; Miyagishi and Taira, 2002; Paul et al., 2002; Sui et al., 2002; Yu et al., 2002; Shen et al., 2003; Zhao et al., 2003; Hosono et al., 2004).

In the present study, we established an optimal fiber-modified Ad vector for transduction of 3T3-L1 preadipocytes and adipocytes and demonstrated that the fiber-modified Ad vector expressing short hairpin RNA (shRNA) against PPARγ efficiently suppressed the differentiation of preadipocytes into adipocytes in 3T3-L1 cells.

2. Materials and methods

2.1. Cells

293 cells and 3T3-L1 cells (clonal subline of the mouse 3T3 that accumulate large amounts of triglyceride fat when the cells are in the resting state; Human Science Research Resources Bank, Japan, JCRB9014) were cultured with Dulbecco's Modified Eagle's Medium supplemented with 10% fetal calf serum (FCS). NIH3T3 cells were cultured with minimum essential medium supplemented with 10% FCS.

2.2. Construction of stable CAR-expressing NIH3T3 cells

Mouse liver total RNA was isolated using ISOGEN reagent (Nippon Gene, Tokyo, Japan) according to the manufacturer's instructions. Mouse liver cDNA was obtained from reverse transcription (RT) product for mouse liver total RNA using a SuperScript First-Strand Synthesis System for RT-PCR (Invitrogen Life Technologies, Carlsbad, CA, USA) according to the manufacturer's instructions. Mouse CAR cDNA was amplified from mouse liver cDNA using the following primers: 5′-accatggcgcgcc-tactgtgct-3′ and 5′-ttcagtagtccttcatatttat -3′. The amplified polymerase chain reaction (PCR) product was inserted into the TA cloning vector pGEM-T Easy (Promega Corp., Madison, WI, USA) to generate pGEM-T-mCAR. CAR-expressing plasmid pCMV-mCAR was constructed by ligation of the *Eco*RI site of pcDNA3 (Invitrogen Life Technologies) with the *Eco*RI fragment of pGEM-T-mCAR, and was transfected into NIH3T3 cells by SuperFect transfection reagent (Qiagen, Inc., Valencia, CA, USA). The stable CAR-expressing cells, NIH3T3-CAR, were obtained by geneticin (G418) selection.

2.3. Plasmid and virus

pHMCA-LacZ1 contains a β-actin promoter/CMV enhancer with a β-actin intron, which was kindly provided by Dr. J. Miyazaki (Osaka University, Osaka, Japan) (Niwa et al., 1991), an *Escherichia coli* β-galactosidase (LacZ)

gene derived from pCMVβ (Clontech, Palo Alto, CA, USA), and a bovine growth hormone polyadenylation signal, flanked by *I-Ceu*I and *PI-Sce*I sites.

pHM5-H1-PPARγ was constructed by insertion of the oligonucleotides (5′-gatccccgtctgctgatctgcgagccttcaagagaggctcgcagatcagcagacttttttggaaat-3′ and 5′-ctagatttccaaaaagtctgctgatctgcgagcctctcttgaaggctcgcagatcagcagacgggg-3′) (Katayama et al., 2004) (loop sequences were underlined) into the *Bgl*II and *Xba*I sites of pHM5-H1 (Hosono et al., 2004), which is designed to express shRNA upon the insertion of an appropriate sequence into the *Bgl*II/*Xba*I site. pHM5-H1-Scramble was constructed by insertion of the oligonucleotides (5′-gatccccacgctgagtacttcgaaatttcaagagaatttcgaagtactcagcgtttttttggaaat-3′ and 5′-ctagatttccaaaaaaacgctgagtacttcgaaatttctcttgaaatttcgaagtactcagcgggg-3′) (loop sequences were underlined) into the *Bgl*II and *Xba*I sites of pHM5-H1. The sequence was verified on a DNA sequencer (ABI PRISM 310, Applied Biosystems, Foster City, CA, USA).

Ad vectors expressing LacZ or siRNA were constructed by an improved in vitro ligation method (Mizuguchi and Kay, 1998; Mizuguchi and Kay, 1999). Briefly, pHMCA-LacZ1 was digested with *I-Ceu*I and *PI-Sce*I, and then ligated with *I-Ceu*I/*PI-Sce*I-digested pAdHM4 (Mizuguchi and Kay, 1998), pAdHM15-RGD (Mizuguchi et al., 2001), pAdHM41-K7(C) (Koizumi et al., 2003), or pAdHM34 (Mizuguchi and Hayakawa, 2002), resulting in pAdHM4-CALacZ1, pAdHM15-RGD-CALacZ1, pAdHM41-K7-CALacZ1, or pAdHM34-CALacZ1, respectively. pAdHM41-K7-H1, pAdHM41-K7-H1-PPARγ, and pAdHM41-K7-Scramble were constructed by the ligation of *I-Ceu*I/*PI-Sce*I-digested pHM5-H1, pHM5-H1-PPARγ, or pHM5-H1-Scramble, respectively, with *I-Ceu*I/*PI-Sce*I-digested pAdHM41-K7(C).

To generate the virus (Ad-CALacZ, AdRGD-CALacZ, AdF35-CALacZ, AdK7-CALacZ, AdK7-H1, AdK7-H1-PPARγ, AdK7-H1-Scramble), *Pac*I-digested Ad vector plasmids (pAdHM4-CALacZ1, pAdHM15-RGD-CALacZ1, pAdHM34-CALacZ1, pAdHM41-K7-CALacZ1, pAdHM41-K7-H1, pAdHM41-K7-H1-PPARγ, and pAdHM41-K7-Scramble, respectively) were transfected into 293 cells plated in a 60-mm dish with SuperFect (Qiagen, Inc.) according to the manufacturer's instructions. Viruses were prepared as described previously (Mizuguchi and Kay, 1998). AdK7-Null contains no transgene in the E1 deletion region. The virus was purified by $CsCl_2$ gradient centrifugation, dialyzed with the solution containing 10 mM Tris (pH 7.5), 1 mM $MgCl_2$ and 10% glycerol, and stored in aliquots at −70 °C. The determination of virus particle titer was accomplished spectrophotometrically by the method of Maizel et al. (1968).

2.4. X-gal staining

In the case of 3T3-L1 preadipocytes, 3T3-L1 cells (1×10^5 cells) were seeded into a 12-well plates. On the following day, they were transduced with Ad-CALacZ, AdRGD-CALacZ, AdF35-CALacZ, or AdK7-CALacZ (3000 or 10,000 vector particles (VP)/cell) for 1.5 h. Forty-eight hours later, LacZ production in the cells was determined by X-gal (5-bromo-4-chloro-3-indolyl-β-D-galactopyranoside) staining.

In the case of 3T3-L1 adipocytes, 3T3-L1 cells were differentiated as described in the next section. After 6 days in culture with differentiation medium, the cells were transduced with each Ad vector (3000 or 10,000 vector particles (VP)/cell) for 1.5 h. Forty-eight hours later, LacZ production in the cells was determined by X-gal staining.

2.5. Adipocyte differentiation

Induction of adipocyte differentiation was performed as previously described (Tontonoz et al., 1994a). Two days after confluence (day 0), the medium was replaced with differentiation medium containing pioglitazone (CALBIOCHEM, San Diego, CA, USA) (3 μM), insulin (Sigma, Saint Louis, MO, USA) (150 nM), dexamethasone (Sigma) (1 μM) and 3-isobutyl-1-methylxanthine (Sigma) (100 μM), which was changed every 3 days thereafter until analysis.

Differentiation of 3T3-L1 preadipocytes to adipocytes was monitored by measurement of intracellular lipid accumulation using Oil red O staining and glycerol-3-phosphate dehydrogenase (GPDH) activity on day 9. The cells were fixed for 2 h with 10% formaldehyde in isotonic phosphate buffer and then washed with distilled water. The cells were then stained with complete immersion in a

Table 1
Adenovirus vectors used in this study

Name	Fiber type	Gene of interest
Ad-CALacZ	type 5 fiber	CA promoter+LacZ
AdRGD-CALacZ	RGD peptide in the HI-loop of the fiber knob	CA promoter+LacZ
AdK7-CALacZ	polylysine peptide in the C-terminal of the fiber knob	CA promoter+LacZ
AdF35-CALacZ	chimeric type 5 fiber tail and type 35 fiber knob and shaft	CA promoter+LacZ
AdK7-H1	polylysine peptide in the C-terminal of the fiber knob	H1 promoter
AdK7-H1-PPARγ	polylysine peptide in the C-terminal of the fiber knob	H1 promoter+shRNA for PPARγ
AdK7-H1-Scramble	polylysine peptide in the C-terminal of the fiber knob	H1 promoter+shRNA for Scramble
AdK7-Null	polylysine peptide in the C-terminal of the fiber knob	none

CA promoter: β-actin promoter/CMV enhancer with β-actin intron.

working solution (0.3%) of Oil red O for 4 h. Excess dye was removed by exhaustive washing with water. The GPDH activity was measured using a GPDH assay kit (Hokudo, Hokkaido, Japan).

2.6. Reverse transcription–polymerase chain reaction for CAR mRNAs

Total RNA was isolated using ISOGEN reagent according to the manufacturer's instructions. RT was carried out using a SuperScript First-Strand Synthesis System for reverse transcription–polymerase chain reaction (RT-PCR) according to the manufacturer's instructions. PCR amplification of the mouse CAR and GAPDH was performed in 50 μl of a solution containing 1 μl of RT products, 1 U TaKaRa Ex Taq HS and attached reagents (TaKaRa, Shiga, Japan). The sequences of the primer for PCR are as follows: CAR: forward, 5′-aattcctgctgaccgttctt-3′; reverse, 5′-tttctgccagccatggcgta-3′; GAPDH: forward, 5′-accacagtccatgccatcac-3′; reverse, 5′-tccaccaccctgttgctgta-3′. The following parameters were used: CAR: 20 s at 94 °C, 10 s at 60 °C, and 60 s at 72 °C for 35 cycles; GAPDH: 20 s at 94 °C, 10 s at 60 °C, and 60 s at 72 °C for 25 cycles. The PCR products were electrophoresed in 2.0% agarose gel. The sequence of the PCR products was confirmed by direct sequencing.

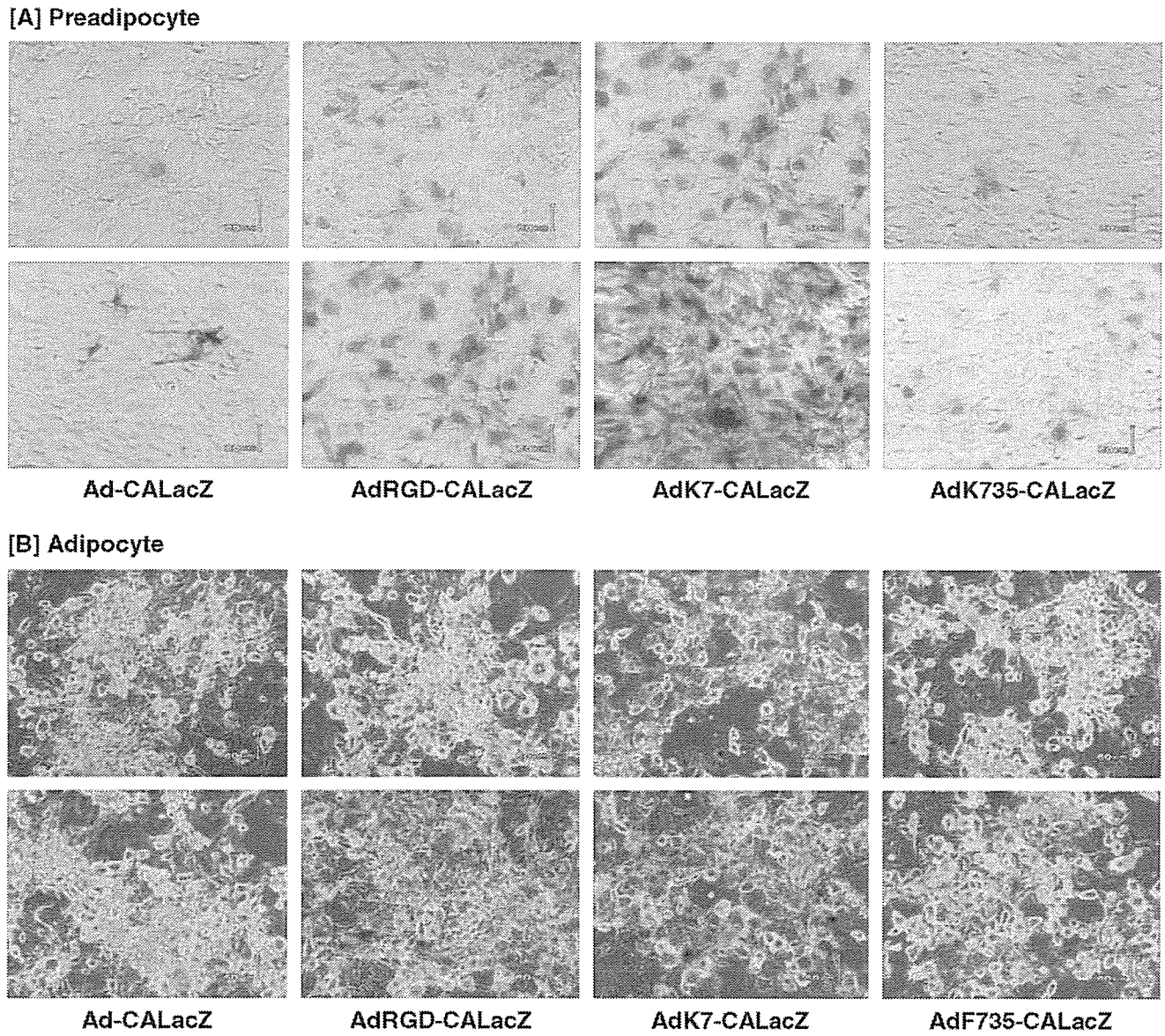

Fig. 1. Comparison of the transduction efficiency of various types of fiber-modified Ad vector into 3T3-L1 preadipocytes and adipocytes. 3T3-L1 preadipocytes (A) and adipocytes (B), which were cultured in differentiation medium containing pioglitazone, insulin, dexamethasone and 3-isobutyl-1-methylxanthine for 6 days, were transduced with Ad-CALacZ, AdRGD-CALacZ, AdK7-CALacZ or AdF35-CALacZ (3000 or 10,000 VP/cells) for 1.5 h. After 48 h in culture, LacZ expression was determined by X-gal staining.

2.7. Western blotting for PPARγ proteins

The cell extracts were prepared in lysis buffer (25 mM Tris [pH 7.5], 1% Triton X-100, 0.5% sodium deoxycholate, 5 mM EDTA, 150 mM NaCl) containing a cocktail of protease inhibitors (Sigma). The protein content was measured with a Bio-Rad assay kit (Bio-Rad, Hercules, CA, USA) using bovine serum albumin as the standard. The protein samples (10 μg) were electrophoresed on 12.5% SDS–polyacrylamide gels under reducing conditions, followed by electrotransfer to Immobilon-P membranes (Millipore, Bedford, MA, USA). After blocking in Block Ace (Dainippon Pharmaceuticals, Osaka, Japan), the filters were incubated with antibodies against PPARγ (Santa Cruz Biotechnology, Inc., Santa Cruz, CA, USA) and GAPDH (Trevigen, Gaithersburg, MD, USA), followed by incubation in the presence of peroxidase-labeled horse anti-mouse IgG antibody (Cell Signaling Technology, Inc., Beverly, MA, USA) or peroxidase-labeled goat anti-rabbit IgG antibody (Cell Signaling Technology, Inc.). The filters were developed using chemiluminescence (ECL Western blotting detection system; Amersham Biosciences, Piscataway, NJ, USA). The signals were read using a LAS-3000 (FUJIFILM, Tokyo, Japan), and quantified by Image Gauge Software (FUJIFILM).

3. Results

3.1. Optimization of fiber-modified Ad vectors for the transduction of 3T3-L1 adipocytes and preadipocytes

The Ad vector is known to transduce 3T3-L1 preadipocytes with very low efficiency (Orlicky et al., 2001; Orlicky and Schaack, 2001; Ross et al., 2003). Therefore, we first optimized the transduction of 3T3-L1 adipocytes as well as preadipocytes by means of fiber-modified Ad vectors, which exhibit different tropism with the conventional Ad vector.

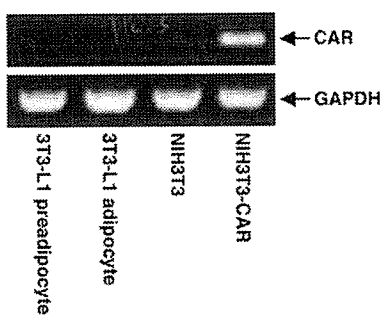

Fig. 2. RT-PCR analysis of CAR mRNA expression in 3T3-L1 preadipocytes and adipocytes. Total RNA was isolated from 3T3-L1 preadipocytes and adipocytes differentiated for 6 days, and RT-PCR analysis was performed as described in Materials and methods. NIH3T3 and NIH3T3-CAR cells were also analyzed as a negative and positive control of CAR mRNA expression, respectively.

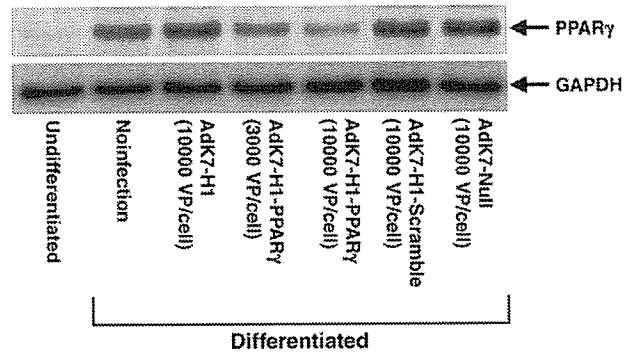

Fig. 3. Suppression of PPARγ expression in 3T3-L1 cells transduced with AdK7-H1-PPARγ. 3T3-L1 preadipocytes were transduced with each Ad vector for 1.5 h. On the following day, the cells reached confluence. From 3 days after Ad treatment, the cells were cultured with differentiation medium containing pioglitazone, insulin, dexamethasone and 3-isobutyl-1-methylxanthine for 4 days. Proteins were then extracted from the cells, and the levels of PPARγ expression were examined by Western blotting. The GAPDH bands served as an internal control for equal total protein loading.

The 3T3-L1 preadipocytes were infected with LacZ-expressing Ad vectors containing modified fiber proteins (Ad-CALacZ, AdRGD-CALacZ, AdF35-CALacZ and AdK7-CALacZ) (Table 1 and Fig. 1A). Ad-CALacZ contains the wild-type fiber, AdRGD-CALacZ contains an RGD peptide motif in the HI-loop of the fiber knob, AdK7-CALacZ contains a polylysine peptide in the C-terminal of the fiber knob, and AdF35-CALacZ contains a fiber protein derived from Ad type 5 fiber tail and Ad type 35 fiber knob and shaft. As shown previously (Orlicky et al., 2001; Orlicky and Schaack, 2001; Ross et al., 2003), Ad-CALacZ was inefficient for transduction of 3T3-L1 preadipocytes. AdK7-CALacZ was the most effective in transducing the LacZ genes. Nearly 100% of 3T3-L1 preadipocytes were transduced by AdK7-CALacZ at 10,000 vector particles (VP)/cell. AdRGD-CALacZ mediated higher levels of LacZ expression than Ad-CALacZ but lower levels than AdK7-CALacZ, while AdF35-CALacZ was ineffective.

We then examined the transduction efficiency of 3T3-L1 adipocytes using various types of Ad vectors. 3T3-L1 preadipocytes differentiate into mature, lipid droplet-containing adipocytes when stimulated with an appropriate hormonal cocktail containing insulin, dexamethasone and 3-isobutyl-1-methylxanthine. Pioglitazone, the ligand of PPARγ, enhances adipocyte differentiation of 3T3-L1 cells. 3T3-L1 preadipocytes were cultured with a differentiation medium containing pioglitazone for 6 days and then transduced with Ad vectors (Fig. 1B). Under the differentiated conditions, AdK7-CALacZ showed high transduction efficiency (67% LacZ-positive cells), although its efficiency was slightly lower than that in 3T3-L1 preadipocytes. AdRGD-CALacZ also showed high transduction efficiency (59% LacZ-positive cells). Ad-CALacZ and AdF35-CALacZ were ineffective. No cytotoxicity or other negative effects on cell function were observed in either 3T3-L1 preadipocytes or adipocytes.

To determine why the wild-type Ad vector exhibited inefficient transduction of 3T3-L1 preadipocytes and adipocytes, we examined the expression of CAR, a primary Ad receptor, in 3T3-L1 preadipocytes and adipocytes by RT-PCR analysis (Fig. 2). NIH3T3 and NIH3T3-CAR cells, which are transfectants of the mouse CAR gene, were used as a negative and positive control, respectively. The results showed that CAR mRNA was not present in either 3T3-L1 preadipocytes or adipocytes, suggesting that Ad vectors containing wild-type fiber did not mediate transduction probably due to little expression of CAR. From these results, we concluded that fiber-modification with K7 peptides improved the efficiency of Ad transduction into both 3T3-L1 preadipocytes and adipocytes.

3.2. Suppression of the expression levels of PPARγ in 3T3-L1

Next, we constructed AdK7-H1-PPARγ, which expresses siRNA for PPARγ with K7 peptides-modified fiber knob, and examined whether AdK7-H1-PPARγ inhibited the differentiation of 3T3-L1 preadipocytes into adipocytes. The target

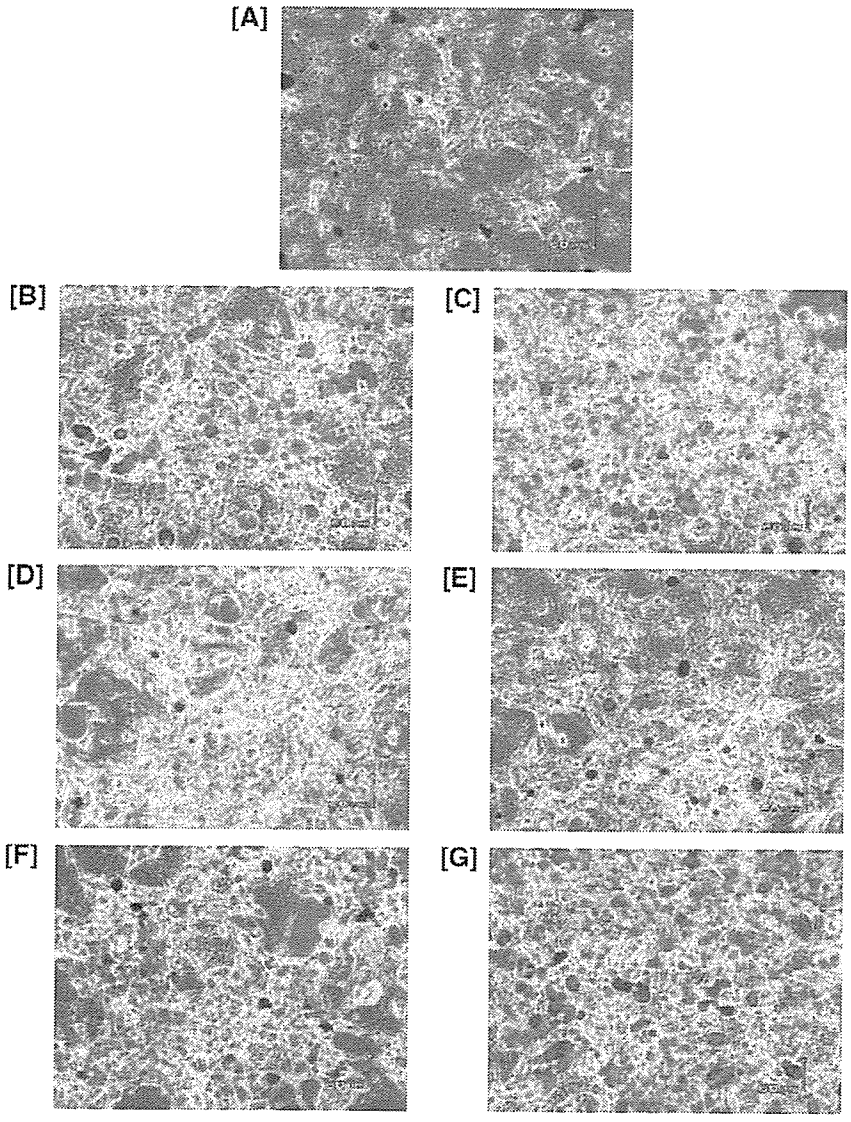

Fig. 4. Suppression of preadipocyte-to-adipocyte differentiation by transduction with AdK7-H1-PPARγ. 3T3-L1 preadipocytes were transduced with each Ad vector for 1.5 h. On the following day, the cells reached confluence. From 3 days after Ad treatment, the cells were cultured with differentiation medium containing pioglitazone, insulin, dexamethasone and 3-isobutyl-1-methylxanthine for 9 days. Then, the intracellular lipid accumulation, which was used as the marker of preadipocyte-to-adipocyte differentiation, was determined by Oil red O staining. (A) 3T3-L1 preadipocytes (3T3-L1 cells cultured with normal medium); (B) 3T3-L1 adipocytes (3T3-L1 cells cultured with differentiation medium without Ad treatment); (C) 3T3-L1 cells cultured with differentiation medium with AdK7-H1 (10,000 VP/cell) treatment; (D) 3T3-L1 cells cultured with differentiation medium with AdK7-H1-PPARγ (3000 VP/cell) treatment; (E) 3T3-L1 cells cultured with differentiation medium with AdK7-H1-PPARγ (10,000 VP/cell) treatment; (F) 3T3-L1 cells cultured with differentiation medium with AdK7-H1-Scramble (10,000 VP/cell) treatment; (G) 3T3-L1 cells cultured with differentiation medium with AdK7-Null (10,000 VP/cell) treatment.

sequence of siRNA for PPARγ was selected to knockdown both PPARγ1 and PPARγ2 (Katayama et al., 2004). We confirmed by Western blotting that AdK7-H1-PPARγ suppresses the expression levels of PPARγ in 3T3-L1 adipocytes (Fig. 3). The levels of PPARγ in the cells treated with 3000 or 10,000 VP/cell of AdK7-H1-PPARγ were decreased to 51% or 16% of the levels in cells treated with AdK7-Null (10,000 VP/cells), respectively. AdK7-H1, AdK7-H1-Scramble and AdK7-Null did not show any effect on the PPARγ expression, compared with non-infected cells. These results indicated that AdK7-H1-PPARγ effectively suppressed the expression of PPARγ in 3T3-L1 cells.

3.3. Suppression of the preadipocyte-to-adipocyte differentiation in 3T3-L1 cells

During the process of preadipocyte-to-adipocyte differentiation, 3T3-L1 preadipocytes initiate the storage of energy in the form of triacylglycerol-rich lipid droplets. The degree of differentiation of 3T3-L1 cells can be evaluated by measuring the accumulation of intracellular lipids, which are stained by Oil red O, and GPDH activity. We next examined whether AdK7-H1-PPARγ suppresses the preadipocyte-to-adipocyte differentiation in 3T3-L1 cells. The 3T3-L1 cells were transduced with Ad vectors and reached confluence on the following day. Two days after reaching confluence, the cells were cultured with differentiation medium for 9 days and stained with Oil red O. Intracellular lipid accumulation was reduced in 3T3-L1 cells transduced with AdK7-H1-PPARγ (Fig. 4). The levels of GPDH activity in the cells treated with 3000 or 10,000 VP/cell of AdK7-H1-PPARγ were decreased to 55% or 33% of the levels in cells treated with AdK7-Null (10,000 VP/cell), respectively (Fig. 5). AdK7-H1, AdK7-H1-Scramble and AdK7-Null did not show any suppressive effect on the accumulation of intracellular lipid and GPDH activity (Fig. 5). These results suggested that AdK7-H1-PPARγ efficiently suppressed the preadipocyte-to-adipocyte differentiation of 3T3-L1 cells.

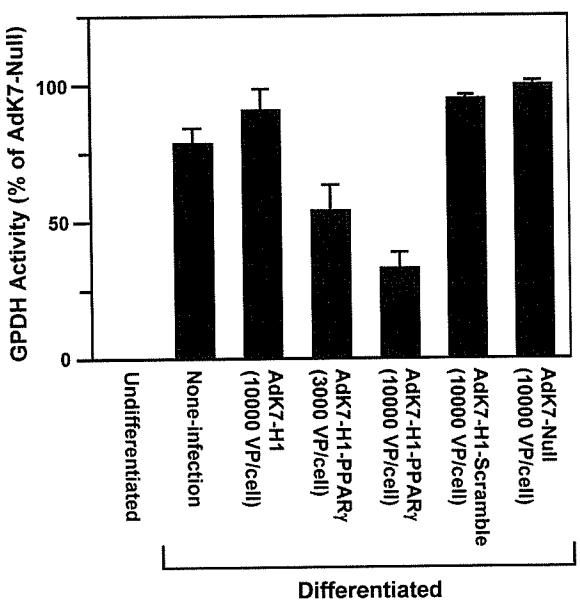

Fig. 5. Suppression of the fatty synthesis on 3T3-L1 cells transduced with AdK7-H1-PPARγ. The cells and virus were treated as described in the legends of Fig. 4. The fatty synthesis was determined by the measurement of GPDH activity in 3T3-L1 cells. Data were expressed as percentage of the GPDH activity of 3T3-L1 cells cultured with differentiation medium with AdK7-Null (10,000 VP/cell) treatment.

4. Discussion

3T3-L1 cell line is widely used for studying adipocyte differentiation and adipose biology. However, this cell line is poorly transduced by the conventional Ad vectors or DNA transfection reagents. In the present study, we successfully transduced nearly 100% of 3T3-L1 preadipocytes by using fiber-modified Ad vectors containing polylysine peptides and showed that Ad vector-mediated RNAi for PPARγ efficiently suppressed the preadipocyte-to-adipocyte differentiation. We also showed that 3T3-L1 adipocytes were efficiently transduced by the fiber-modified Ad vectors containing polylysine peptides. Carlotti et al. reported that Ad vector-mediated gene transfer into 3T3-L1 adipocytes was associated with marked cytopathogenicity (Carlotti et al., 2004). In our results, no cytotoxicity, adipogenicity, or other negative effects on cell function were observed by the Ad vector-mediated gene transfer.

Several strategies have been employed to overcome the poor transduction efficiency of 3T3-L1 cells. Because the low expression of CAR, the primary Ad receptor, in 3T3-L1 cells would the cause of the poor transduction of the conventional Ad vectors (Fig. 2), 3T3-L1 cells stably expressing CAR by the transfection have been developed (Orlicky et al., 2001; Ross et al., 2003). However, CAR is an adhesion molecule which mediates tight junctions and homotypic interactions (Honda et al., 2000; Cohen et al., 2001). Therefore, there might be negative effects of ectopic CAR expression in the process of adipogenesis of 3T3-L1 cells. Another strategy is to use transduction-enhancing agents such as polylysine, lipofectAMINE (Invitrogen Life Technologies), or SuperFect (Qiagen Inc.), which mediate CAR-independent transduction of Ad vectors (Orlicky and Schaack, 2001). These reagents sometimes negatively affect cellular function, e.g., via their cytotoxicity or their inhibition of cell growth and differentiation. Complexes of Ad vectors and transduction-enhancing agents are also non-uniform and are not likely to show reproducible results. Fiber-modified Ad vectors overcome all these problems. Among the vectors tested in the present study, polylysine-modification of the Ad fiber, which is negatively charged, exhibited the most efficient gene transfer to 3T3-L1 preadipocytes and adipocytes. This result correlates well with the report of Orlicky and Schaack that complexes of Ad vectors and polylysine enhanced transduction in 3T3-L1

cells (Orlicky and Schaack, 2001), although the vector in the present study contained fiber that was genetically modified with polylysine (a stretch of seven lysine residues), while their vector is just a complex of Ad and polylysine. 3T3-L1 cells might produce a large number of negatively charged glycosaminoglycans.

PPARγ is a master regulator of adipogenesis and plays an important role in the regulation of insulin sensitivity and glucose homeostasis (Tontonoz et al., 1994b; Wu et al., 1998; Kubota et al., 1999; Berger and Moller, 2002). The inhibition of preadipocyte-to-adipocyte differentiation by the silencing of PPARγ expression in 3T3-L1 cells suggests that the fiber-modified Ad vector-mediated RNAi could be widely used for the basic study of adiposity and diabetes.

Homozygous PPARγ-null mice are embryonically lethal due to placental dysfunction. Heterozygous mice ($PPAR\gamma^{+/-}$) and conditional knockout mice have been used to study the function of PPARγ under in vivo conditions (Kubota et al., 1999). However, generation of these mice is time-consuming. In the heterozygous mice ($PPAR\gamma^{+/-}$), the expression levels of $PPAR\gamma^{+/-}$ cannot be regulated and are half those of the wild-type mice. Since the Ad vectors mediate efficient gene transduction even under in vivo conditions, conditional PPARγ knockdown mice might be generated by the direct in vivo injection of Ad vectors containing the siRNA expression cassette for PPARγ. Knockdown levels of PPARγ expression could be regulated by adjusting the dose of the vector. Koo et al. recently produced PGC-1 (PPARγ coactivator-1) knockdown mice by Ad delivery of PGC-1 RNAi to the liver (Koo et al., 2004).

In conclusion, the fiber-modified Ad vectors containing polylysine peptides mediate efficient gene transfer into 3T3-L1 preadipocytes and adipocytes. RNAi of PPARγ by the delivery of modified Ad vectors suppresses the preadipocyte-to-adipocyte differentiation in 3T3-L1 cells. Ad vector-mediated RNAi for PPARγ should be useful for not only studying the biological and physiological mechanism of PPARγ during adipogenesis in adiposity and diabetes, but also in therapeutic application to these and other diseases.

Acknowledgements

We thank Takashi Fukushima for technical assistance and Koichiro Wada (Osaka University) for helpful discussion. T.H. is a recipient of a fellowship from the Japan Society for the Promotion of Science. This work was supported by grants from the Ministry of Health, Labour, and Welfare of Japan and a Grant-in-Aid for Scientific Research on Priority Areas of the Ministry of Education, Culture, Sports, Science and Technology (MEXT) of Japan.

References

Berger, J., Moller, D.E., 2002. The mechanisms of action of PPARs. Annu. Rev. Med. 53, 409–435.

Brummelkamp, T.R., Bernards, R., Agami, R., 2002. A system for stable expression of short interfering RNAs in mammalian cells. Science 296, 550–553.

Carlotti, F., et al., 2004. Lentiviral vectors efficiently transduce quiescent mature 3T3-L1 adipocytes. Mol. Ther. 9, 209–217.

Cohen, C.J., Shieh, J.T., Pickles, R.J., Okegawa, T., Hsieh, J.T., Bergelson, J.M., 2001. The coxsackievirus and adenovirus receptor is a transmembrane component of the tight junction. Proc. Natl. Acad. Sci. U. S. A. 98, 15191–15196.

Dmitriev, I., et al., 1998. An adenovirus vector with genetically modified fibers demonstrates expanded tropism via utilization of a coxsackievirus and adenovirus receptor-independent cell entry mechanism. J. Virol. 72, 9706–9713.

Elbashir, S.M., Harborth, J., Lendeckel, W., Yalcin, A., Weber, K., Tuschl, T., 2001. Duplexes of 21-nucleotide RNAs mediate RNA interference in cultured mammalian cells. Nature 411, 494–498.

Gaggar, A., Shayakhmetov, D.M., Lieber, A., 2003. CD46 is a cellular receptor for group B adenoviruses. Nat. Med. 9, 1408–1412.

Gregoire, F.M., Smas, C.M., Sul, H.S., 1998. Understanding adipocyte differentiation. Physiol. Rev. 78, 783–809.

Havenga, M.J., et al., 2001. Improved adenovirus vectors for infection of cardiovascular tissues. J. Virol. 75, 3335–3342.

Honda, T., et al., 2000. The coxsackievirus-adenovirus receptor protein as a cell adhesion molecule in the developing mouse brain. Brain Res. Mol. Brain Res. 77, 19–28.

Hosono, T., et al., 2004. Adenovirus vector-mediated doxycycline-inducible RNA interference. Hum. Gene Ther. 15, 813–819.

Katayama, K., et al., 2004. RNA interfering approach for clarifying the PPARgamma pathway using lentiviral vector expressing short hairpin RNA. FEBS Lett. 560, 178–182.

Koizumi, N., Mizuguchi, H., Utoguchi, N., Watanabe, Y., Hayakawa, T., 2003. Generation of fiber-modified adenovirus vectors containing heterologous peptides in both the HI loop and C terminus of the fiber knob. J. Gene Med. 5, 267–276.

Koo, S.H., et al., 2004. PGC-1 promotes insulin resistance in liver through PPAR-alpha-dependent induction of TRB-3. Nat. Med. 10, 530–534.

Krasnykh, V.N., Mikheeva, G.V., Douglas, J.T., Curiel, D.T., 1996. Generation of recombinant adenovirus vectors with modified fibers for altering viral tropism. J. Virol. 70, 6839–6846.

Kubota, N., et al., 1999. PPAR gamma mediates high-fat diet-induced adipocyte hypertrophy and insulin resistance. Mol. Cell 4, 597–609.

Maizel Jr., J.V., White, D.O., Scharff, M.D., 1968. The polypeptides of adenovirus: I. Evidence for multiple protein components in the virion and a comparison of types 2, 7A, and 12. Virology 36, 115–125.

McManus, M.T., Sharp, P.A., 2002. Gene silencing in mammals by small interfering RNAs. Nat. Rev. Genet. 3, 737–747.

Miyagishi, M., Taira, K., 2002. U6 promoter-driven siRNAs with four uridine 3′ overhangs efficiently suppress targeted gene expression in mammalian cells. Nat. Biotechnol. 20, 497–500.

Mizuguchi, H., Hayakawa, T., 2002. Adenovirus vectors containing chimeric type 5 and type 35 fiber proteins exhibit altered and expanded tropism and increase the size limit of foreign genes. Gene 285, 69–77.

Mizuguchi, H., Kay, M.A., 1998. Efficient construction of a recombinant adenovirus vector by an improved in vitro ligation method. Hum. Gene Ther. 9, 2577–2583.

Mizuguchi, H., Kay, M.A., 1999. A simple method for constructing E1- and E1/E4-deleted recombinant adenoviral vectors. Hum. Gene Ther. 10, 2013–2017.

Mizuguchi, H., et al., 2001. A simplified system for constructing recombinant adenoviral vectors containing heterologous peptides in the HI loop of their fiber knob. Gene Ther. 8, 730–735.

Niwa, H., Yamamura, K., Miyazaki, J., 1991. Efficient selection for high-expression transfectants with a novel eukaryotic vector. Gene 108, 193–199.

Ntambi, J.M., Young-Cheul, K., 2000. Adipocyte differentiation and gene expression. J. Nutr. 130, 3122S–3126S.

Orlicky, D.J., Schaack, J., 2001. Adenovirus transduction of 3T3-L1 cells. J. Lipid Res. 42, 460–466.

Orlicky, D.J., DeGregori, J., Schaack, J., 2001. Construction of stable coxsackievirus and adenovirus receptor-expressing 3T3-L1 cells. J. Lipid Res. 42, 910–915.

Paul, C.P., Good, P.D., Winer, I., Engelke, D.R., 2002. Effective expression of small interfering RNA in human cells. Nat. Biotechnol. 20, 505–508.

Ross, S.A., Song, X., Burney, M.W., Kasai, Y., Orlicky, D.J., 2003. Efficient adenovirus transduction of 3T3-L1 adipocytes stably expressing coxsackie-adenovirus receptor. Biochem. Biophys. Res. Commun. 302, 354–358.

Segerman, A., Atkinson, J.P., Marttila, M., Dennerquist, V., Wadell, G., Arnberg, N., 2003. Adenovirus type 11 uses CD46 as a cellular receptor. J. Virol. 77, 9183–9191.

Shayakhmetov, D.M., Papayannopoulou, T., Stamatoyannopoulos, G., Lieber, A., 2000. Efficient gene transfer into human CD34(+) cells by a retargeted adenovirus vector. J. Virol. 74, 2567–2583.

Shen, C., Buck, A.K., Liu, X., Winkler, M., Reske, S.N., 2003. Gene silencing by adenovirus-delivered siRNA. FEBS Lett. 539, 111–114.

Short, J.J., Pereboev, A.V., Kawakami, Y., Vasu, C., Holterman, M.J., Curiel, D.T., 2004. Adenovirus serotype 3 utilizes CD80 (B7.1) and CD86 (B7.2) as cellular attachment receptors. Virology 322, 349–359.

Sui, G., Soohoo, C., Affarel, B., Gay, F., Shi, Y., Forrester, W.C., 2002. A DNA vector-based RNAi technology to suppress gene expression in mammalian cells. Proc. Natl. Acad. Sci. U. S. A. 99, 5515–5520.

Tontonoz, P., Hu, E., Graves, R.A., Budavari, A.I., Spiegelman, B.M., 1994a. mPPAR gamma 2: tissue-specific regulator of an adipocyte enhancer. Genes Dev. 8, 1224–1234.

Tontonoz, P., Hu, E., Spiegelman, B.M., 1994b. Stimulation of adipogenesis in fibroblasts by PPAR gamma 2, a lipid-activated transcription factor. Cell 79, 1147–1156.

Vidal-Puig, A.J., et al., 1997. Peroxisome proliferator-activated receptor gene expression in human tissues. Effects of obesity, weight loss, and regulation by insulin and glucocorticoids. J. Clin. Invest. 99, 2416–2422.

Wickham, T.J., et al., 1997. Increased in vitro and in vivo gene transfer by adenovirus vectors containing chimeric fiber proteins. J. Virol. 71, 8221–8229.

Wu, Z., Xie, Y., Morrison, R.F., Bucher, N.L., Farmer, S.R., 1998. PPAR gamma induces the insulin-dependent glucose transporter GLUT4 in the absence of C/EBPalpha during the conversion of 3T3 fibroblasts into adipocytes. J. Clin. Invest. 101, 22–32.

Yu, J.Y., DeRuiter, S.L., Turner, D.L., 2002. RNA interference by expression of short-interfering RNAs and hairpin RNAs in mammalian cells. Proc. Natl. Acad. Sci. U. S. A. 99, 6047–6052.

Zhao, L.J., Jian, H., Zhu, H., 2003. Specific gene inhibition by adenovirus-mediated expression of small interfering RNA. Gene 316, 137–141.

0026-895X/05/6703-749–756$20.00
MOLECULAR PHARMACOLOGY

Mol Pharmacol 67:749–756, 2005

Vol. 67, No. 3
8375/1196087
Printed in U.S.A.

A Novel Strategy for the Enhancement of Drug Absorption Using a Claudin Modulator

Masuo Kondoh, Akane Masuyama, Azusa Takahashi, Nagayoshi Asano, Hiroyuki Mizuguchi, Naoya Koizumi, Makiko Fujii, Takao Hayakawa, Yasuhiko Horiguchi, and Yoshiteru Watanbe

Department of Biopharmaceutics and Pharmaceutics, Showa Pharmaceutical University, Tokyo, Japan (M.K., A.M., A.T., N.A., N.K., M.F., Y.W.); Project III, National Institute of Health Sciences, Osaka Branch, Fundamental Research Laboratories for Development of Medicine, Osaka, Japan (H.M.); National Institute of Health Sciences, Tokyo, Japan (T.H.); and Department of Bacterial Toxicology, Research Institute for Microbial Diseases, Osaka University, Osaka, Japan (Y.H.)

Received October 17, 2004; accepted December 14, 2004

ABSTRACT

Claudin, a tight junction integral membrane protein and a family of proteins, forms the actual sealing element of the tight junction. There are more than 20 members of the claudin family with different tissue-specific expression and barrier functions. Thus, a family of claudin may be a target for modifying the absorption of drugs. Here, we examined whether modulation of claudin could be used to enhance drug absorption. In the current studies, we used a C-terminal fragment of *Clostridium perfringens* enterotoxin (C-CPE) as a modulator of claudin-4. The absorption of dextran was assessed in an in situ loop assay in rats to evaluate the absorption-enhancing effects of C-CPE. Treatment with C-CPE dose-dependently enhanced the absorption of dextran (mol. wt. 4000). These effects were not accompanied by injury of the intestinal mucosa as assessed by leakage of lactose dehydrogenase and histological observation. C-CPE was over 400-fold more potent at enhancing dextran absorption than capric acid, a clinically used enhancer of absorption. C-CPE interacted directly with claudin-4, and C-CPE lacking a part the C terminus neither bound claudin-4 nor enhanced absorption in the rat jejunum. These results suggest that C-CPE enhances the absorption of dextran in rat jejunum, apparently through interactions with claudin-4, and this effect may represent an effective novel strategy for enhancing the absorption of drugs.

Recent progress in genomics and proteomics has made it possible to use not only low molecular weight organic compounds but also high molecular weight peptides, proteins, and DNA as drugs for clinical therapy. Efficient delivery is a key issue in the clinical use of these higher molecular weight drugs. Passing across the epithelia is a first key step for absorption of a drug, irrespective of oral, intravenous, and interdermal administration (Powell, 1981). There are two pathways for absorption in epithelia: transcellular and paracellular. The former pathway is mediated by transporters, which are membrane proteins that regulate the cellular influx and efflux of endogenous substrates, including amino acids and fatty acids. Some drugs that mimic endogenous transporter substrates can be taken up through these proteins (Adibi, 1997; Rao et al., 1999; Edwards, 2001). Uptake via the paracellular pathway, on the other hand, is attractive route for the absorption of high molecular weight and large-sized drugs. Conventional methods for taking up molecules via the paracellular pathway include chelating divalent cations and treatment with medium chain fatty acids, including capric acid (C10). These can be toxic in the treated region, and, moreover, the specificity of the absorption-enhancing effects are very poor (Yamamoto et al., 1996). Thus, the clinical use of these absorption enhancers remains limited.

The primary barrier to the transport of solutes from the apical to the basal side are the tight junctions (TJs), specialized membrane domains located at the most apical region of polarized epithelial and endothelial cells (Mitic et al., 2000; Anderson, 2001). The TJ is a complex of various proteins, including junctional adhesion molecule (JAM), occludin, and claudin. JAM is a junction-associated membrane protein

This work was partly supported by a grant-in-aid from the Ministry of Education, Science and Sports, Japan.
Article, publication date, and citation information can be found at http://molpharm.aspetjournals.org.
doi:10.1124/mol.104.008375.

ABBREVIATIONS: TJ, tight junction; CPE, *Clostridium perfringens* enterotoxin; C-CPE, C-terminal fragment of *Clostridium perfringens* enterotoxin; JAM, junctional adhesion molecule; CPE-R, receptor for *Clostridium perfringens* enterotoxin; FD, fluorescein isothiocyanate-dextran; PBS, phosphate-buffered saline; PAGE, polyacrylamide gel electrophoresis; AUC, area under the plasma concentration-time curve; LDH, lactose dehydrogenase; N-CPE, N-terminal fragment of *Clostridium perfringens*.

with a molecular mass of 40 kDa (Martin-Pardura et al., 1998), and its involvement in the barrier function of the TJ remains unclear. Occludin is an integral membrane protein bearing four transmembrane domains and with a molecular mass of 65 kDa. It is predicted to play a role not only in the structure but also in the barrier function of the TJ (Furuse et al., 1993; Balda et al., 1996; McCarthy et al., 1996; Chen et al., 1997; Wong and Gumbiner, 1997). However, deletion of occludin does not result in disruption of the TJ barrier function (Balda et al., 1996; Saitou et al., 1998), and whether occludin is a major constituent of TJs remains uncertain. In contrast, claudin is now believed to be a major constituent of TJ (Morita et al., 1999; Sonoda et al., 1999; Tsukita and Furuse, 2000; Tsukita et al., 2001; Furuse et al., 2002; Nitta et al., 2003). Claudins, which have molecular masses of ~23 kDa, comprise a multigene family consisting of more than 20 members (Morita et al., 1999; Tsukita et al., 2001). TJ strands are copolymers of heterogeneous claudin species and occludin, and heterogeneous claudin species constitute the backbone of TJ strands in situ (Furuse et al., 1999). It is interesting that the localization and barrier function of each member of the claudin varies among tissues. For example, loss of function of the blood brain-barrier is observed in claudin-5-deficient mice (Nitta et al., 2003), whereas epidermal barrier function is disrupted in claudin-1-deficient mice (Furuse et al., 2002). In addition, in claudin-11-deficient mice, TJs are absent in the Sertoli cells in the testis (Gow et al., 1999). These findings indicate that disruption of claudin function with an inhibitor is a promising means for the tissue-specific enhancement of absorption.

Clostridium perfringens enterotoxin (CPE) is a 35-kDa protein that causes food poisoning in humans (McClane, 1994). The C terminus of CPE (C-CPE) is involved in the binding of CPE to the target cells, whereas the N terminus is involved in its cytotoxicity (Kokai-Kun and McClane, 1997). Katahira et al. (1997) identified the receptor for CPE (CPE-R) and found that CPE-R has significant similarity to the rat androgen withdrawal apoptosis protein RVP1. The biological function of CPE-R and RVP1 remained unknown until Morita et al. (1999) found that CPE-R is claudin-4 and that RVP1 is claudin-3. CPE is cytotoxic to claudin-3- and -4-positive cells, but this effect is lost if its N terminus is removed. It is noteworthy that treatment of the cells with C-CPE reduces the transepithelial electrical resistance, a typical measurement of the barrier function of the TJ (Sonoda et al., 1999). These findings indicate that C-CPE may be a promising lead compound for the development of a novel absorption-enhancing agent. In this study, we investigated whether inhibition of claudin by C-CPE can enhance the absorption of dextran in an in situ loop assay and whether this is mediated by claudin-4.

Materials and Methods

Animals, Cells, and Reagents. Wistar male rats (250–280 g) were obtained from Animal and Material Laboratories, Inc. (Tokyo, Japan). The rats were maintained in an environmentally controlled room (23 ± 1.5°C) with a 12-h light/12-h dark cycle and allowed access to standard rodent chow and water ad libitum. The rats were allowed a period of at least 1 week to adapt. Fluorescein isothiocyanate-dextran (FD) with molecular weights of 4000 (FD-4), 10,000 (FD-10), 20,000 (FD-20), and 40,000 (FD-40) were obtained from Sigma-Aldrich (St. Louis, MO). Anti-claudin-1, -2, -3, -4, and -5 antibodies were purchased from Zymed Laboratories (South San Francisco, CA), and horseradish peroxide-labeled secondary antibodies and anti-His-tag antibody were obtained from Cell Signaling Technology Inc. (Beverly, MA) and Novagen (Madison, WI), respectively. Ni-agarose resin and a Ni-agarose column were obtained from Invitrogen (Carlsbad, CA). All reagents were of research grade.

Purification of C-CPE. C-CPE was purified as described previously (Katahira et al., 1997). In brief, the DNA fragment corresponding to amino acid residues 184 to 319 of CPE was cloned into pET16b vector (Novagen). The C-CPE plasmid (pET16bHis$_{10}$C-CPE) was transfected into *Escherichia coli*. BL21 (DE3) strains and the synthesis of C-CPE were stimulated by addition of isopropyl β-D-thiogalactopyranoside (Wako Pure Chemicals, Osaka, Japan). The cells were harvested, resuspended in buffer A [10 mM Tris-HCl, pH 8.0, 400 mM NaCl, 5 mM $MgCl_2$, 10% glycerol, 0.1 mM (*p*-amidinophenyl)methanesulfonyl fluoride hydrochloride, and 1 mM β-mercaptoethanol], and then lysed by sonication. The lysates were applied to the Ni-column, and C-CPE bound to the Ni-resin was eluted with a 0 to 400 mM imidazole gradient in buffer A. The solvent for C-CPE was changed to phosphate-buffered saline (PBS) by gel filtration using PD-10 column (Amersham Biosciences Inc., Piscataway, NJ), and the resulting C-CPE solution was stored at −80°C until use. The concentration of C-CPE was estimated by a protein assay kit using bovine serum albumin as a standard (Bio-Rad, Hercules, CA). The presence of C-CPE was confirmed by Western blotting with a His-Tag antibody (data not shown).

Preparation of C-Terminal Truncated C-CPE. C-CPE lacking the C-terminal amino acids 290 to 319 (C-CPE289) or 304 to 319 (C-CPE303) were prepared as follows. The C-terminal-deficient C-CPEs were cloned by polymerase chain reaction amplification using pET16bHis$_{10}$C-CPE plasmid as a template, a common sense primer (5′-ctcgagagatgtgttttaacagttcca-3′, underline indicates the XhoI site), and an antisense primer for C-CPE289 (5′-ggatcctatatatcaacataatgatcttt-3′, underline indicates the BamHI site) or C-CPE303 (5′-ggatcctaattagctttcattacaagaac-3′, underline indicates the BamHI site). The resulting C-terminal C-CPE fragment was subcloned into the pGEM T-Easy Vector (Promega, Madison, WI), and the sequences of C-CPE289 and C-CPE303 were confirmed. The XhoI/BamHI fragment of the pTA/C-CPE289 or pTA/C-CPE303 was cloned into the pET16b vector at the XhoI/BamHI site. His-tagged C-CPE289 and C-CPE303 were then purified as described previously with some modifications (Katahira et al., 1997). In brief, pET16b plasmid with C-CPE289 and C-CPE303 was introduced into the *E. coli* BL21 (DE3) strain, and expression of the C-CPE289 and C-CPE303 was induced with 0.1 mM isopropyl β-D-thiogalactopyranoside (Wako Pure Chemicals). The *E. coli* cells were harvested and lysed in buffer A containing 8 M urea. The lysates were centrifuged, and the resulting supernatants were applied to a Ni-NTA resin (Invitrogen). The His-tagged proteins were eluted in a gradient of 0 to 2 M imidazole in buffer A. The purification of the His-tagged C-CPE289 and C-CPE303 were confirmed by SDS-PAGE followed by staining the gels with Coomassie Brilliant Blue and by Western blotting with a His-tag antibody (data not shown).

In Situ Loop Assay. The experimental protocol for in situ loop assay was approved by the ethics committee of Showa Pharmaceutical University. Intestinal absorption of FDs was examined by in situ loop assay as follows. Rats were anesthetized with thiamylal sodium (Mitsubishi Pharma Co. Ltd., Osaka, Japan). A midline abdominal incision was made, and the lumen of the jejunum or colon was washed with saline. A jejunal or colonal loop (5 cm in length) was prepared by closing both ends with sutures. Test samples were dissolved in 200 μl of PBS and then administered into the jejunal or colonal loop. Blood was collected from the carotid vein at the indicated periods. The plasma concentration of FDs was determined with a fluorescence spectrophotometer (Fluoroskan Ascent FL; Thermo Electron Corp., Waltham, MA). The area under the plasma concentration-time curve from 0 to 4 h (AUC_{0-4}) was calculated by the trapezoidal method.